NACA

RESEARCH MEMORANDUM

THE CALCULATION OF CERTAIN STATIC AEROELASTIC

PHENOMENA OF WINGS WITH TIP TANKS OR

BOOM-MOUNTED LIFTING SURFACES

By Franklin W. Diederich and Kenneth A. Foss

Langley Aeronautical Laboratory
Langley Field, Va.

CLASSIFICATION CANCELLED

Author Naca RA 2711 Date 10/12/54

By DWFA 11/8/54 See

NATIONAL ADVISORY COMMITTEE
FOR AERONAUTICS

WASHINGTON
August 27, 1952

UNCLASSIFIED
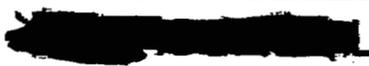
NATIONAL ADVISORY COMMITTEE FOR AERONAUTICS

RESEARCH MEMORANDUM

THE CALCULATION OF CERTAIN STATIC AEROELASTIC

PHENOMENA OF WINGS WITH TIP TANKS OR

BOOM-MOUNTED LIFTING SURFACES

By Franklin W. Diederich and Kenneth A. Foss

SUMMARY

The matrix-integration method of NACA Rep. 1000 for calculating static aeroelastic phenomena is extended to the case of a wing with concentrated aerodynamic forces at the tip due to tip tanks or boom-mounted lifting surfaces. A simplified method of calculation which is based on the concept of the semirigid wing and which utilizes the presumably known aeroelastic characteristics of the wing alone is presented for cases in which the aerodynamic interaction between the concentrated force and the remainder of the wing can be neglected. The modified matrix-integration method has been used to calculate some static aeroelastic characteristics of an unswept wing with a tip tank, and both methods have been used to calculate the characteristics of a 45° sweptback wing with several boom-mounted lifting-surface configurations.

The results of these calculations show that the presence of a tip tank on an unswept wing tends to deteriorate its static aeroelastic characteristics and that a lifting surface geared to the aileron and mounted on a boom ahead of the tip of a sweptback wing may improve the static aeroelastic characteristics of the wing to a sufficient extent to warrant consideration of such a vane as a device for relieving adverse aeroelastic effects.

INTRODUCTION

The matrix-integration method of references 1 and 2 for calculating static aeroelastic effects of swept wings of arbitrary stiffness implies, as do most other methods of static aeroelastic analysis which treat the wing essentially as a simple beam, that the vertical shear, moment, and torque at the tip are zero. The presence of concentrated forces and moments at the wing tip violates this assumption to the extent that

they are discontinuous at the tip. One case in which such forces are
of interest is a wing with a tip tank. Another case is a wing with a
boom-mounted lifting surface.

This combination may be of interest because a surface mounted on a
boom ahead of the tip of a sweptback wing introduces large twisting
moments and, if the surface is mounted such that its angle of attack is
the same as that of the wing tip, it causes twisting of the structure
in a direction such as to oppose the effect of the bending deformations;
hence, by reducing the net change of angle of attack due to wing defor-
mation the vane tends to reduce the shift of the aerodynamic center due
to aeroelastic action. Since aerodynamic forces due to an aileron
deflection cause twisting and bending deformations both of which give
rise to aerodynamic forces which tend to oppose those due to the aileron
deflection, increasing the twisting deformation by means of a boom-
mounted surface only tends to aggravate the loss of lateral control due
to aileron deflection. However, if the surface is geared to the aileron,
so that it pitches up when the aileron is deflected downward, it tends
to reduce the amount of lateral control lost because of aeroelastic
action. Furthermore, it may increase the lateral-control power sub-
stantially under certain conditions when there is no aeroelastic action,
as, for instance, when the aileron is relatively ineffective because
of boundary-layer accumulation or because of shock on the wing ahead of
the aileron. Consequently, a boom-mounted geared lifting surface
appears to warrant consideration as a device for alleviating adverse
aeroelastic effects.

For these reasons the method of reference 1 is extended to the
case of concentrated forces at the wing tip in the present paper. In
this modified method, most of the matrices used in the analysis of the
wing alone by the method of reference 1 can also be used in the calcu-
lations for the wing with the concentrated force at the tip. If
aerodynamic-induction effects between the wing proper and the body
producing the concentrated aerodynamic force under consideration are
neglected, a simpler method may be used to calculate the desired aero-
elastic effects. Such a method is also described in this paper; it
consists of correcting the presumably known aeroelastic effects of the
wing alone for the presence of the concentrated force in a manner sug-
gested by the semirigid-wing concept.

In order to illustrate the results obtainable by these methods,
calculations have been made for an unswept wing with and without a tip
tank and for a 45° sweptback wing with and without several boom-mounted
lifting-surface configurations. In the case of the sweptback wing,
calculations have been made both by the matrix-integration and the
simplified methods with substantially identical results. The results
of the calculations are discussed and certain conclusions are drawn; a
knowledge of the method of analysis is not required for an understanding
of this discussion.

SYMBOLS

A	aspect ratio
a	location of local aerodynamic center rearward of leading edge, fraction of chord
$\bar{a}$	location of wing aerodynamic center rearward of leading edge of mean aerodynamic chord, fraction of mean aerodynamic chord
b	wing span
b'	wing span less fuselage width
$C_{1,2,3,4}$	constants defined by equations (58) to (61)
$C'_{2,3,4}$	constants defined by equations (69) to (71)
C_{L_α}	rigid-wing lift-curve slope per radian
C_{l_d}	coefficient of damping in roll (rolling-moment coefficient for linear antisymmetric twist of 1 radian at wing tip)
C_{m_α}	pitching-moment-curve slope per radian
c	chord parallel to free stream
$\bar{c}$	average chord (S/b)
c_l	section lift coefficient (l/qc)
d	distance parallel to free stream between center of pressure of boom-mounted lifting surface and elastic axis
EI	bending stiffness
e	local position of elastic axis rearward of leading edge, fraction of chord
e_1	distance along chord from elastic axis to section aerodynamic center, fraction of chord (see fig. 1)
e_2	distance along chord from elastic axis to center of pressure due to aileron deflection, fraction of chord (see fig. 1)

GJ   torsion stiffness

g, g' factors defined by equations (22) and (33)

K   gear ratio between boom motion and aileron motion

K_B spring constant of boom

$K_{P,R,v}$ coefficients defined by equations (40), (41), and (66)

k   dimensionless parameter $\left(\dfrac{(GJ)_r}{(EI)_r} \dfrac{b'/2}{e_{1_r}\bar{c}} \dfrac{\tan \Lambda}{\cos^2\Lambda}\right)$

$K_{0,2,3,4}$ coefficients defined by equations (68) to (71)

L   lift

l section lift

M   accumulated bending moment (about an axis parallel to free stream, unless specified otherwise)

M_0 free-stream Mach number

P   concentrated normal force

q   dynamic pressure

q^* dimensionless dynamic pressure $\left(\dfrac{C_{L_\alpha}\left(\dfrac{b'}{2}\right)^2 e_{1_r}\bar{c}^2\cos \Lambda}{(GJ)_r} q\right)$

$\bar{q}$ dimensionless dynamic pressure $\left(\dfrac{C_{L_\alpha}\left(\dfrac{b'}{2}\right)^3 \bar{c} \tan \Lambda}{(EI)_r \cos \Lambda} q\right)$

T   accumulated torsion moment (about an axis perpendicular to plane of symmetry, unless specified otherwise)

t   section pitching (or torsion) moment per unit length perpendicular to plane of symmetry

R   concentrated pitching moment or torque

S	wing area
$\overline{V}_t$	volume of tip tank
y	lateral ordinate measured from plane of symmetry
y^*	dimensionless lateral ordinate $\left(\dfrac{y}{b/2}\right)$
α	local angle of attack, radians $(\alpha_s + \alpha_g)$
$\overline{\alpha}$	total angle of attack, including increment due to aeroelastic action, radians
$\Delta\alpha$	angular deformation of boom at lifting surface, radians
α_δ	effective angle of attack due to unit aileron deflection $\left(\dfrac{dc_l/d\delta}{dc_l/d\alpha}\right)$
Γ	local dihedral or spanwise slope of elastic axis, radians
δ	aileron deflection (in planes parallel to plane of symmetry), radians
ϵ	moment-arm ratio $\left(e_2/e_1\right)$
η	lateral distance from wing root
η^*	dimensionless lateral distance $\left(\dfrac{\eta}{b'/2}\right)$
$\kappa = \dfrac{C_{l_d}}{C_{L_\alpha}}$	
Λ	angle of sweepback at elastic axis
λ	taper ratio (Tip chord/Root chord)
φ	angle of twist about elastic axis, radians

Subscripts:

a	pertaining to antisymmetric case or to aileron
BD	at divergence of boom

D   at divergence

g   geometric (built in or due to airplane attitude)

P   due to concentrated normal force

R   at reversal or due to concentrated pitching moment

r   at wing root or reference value

s   due to structural deformation

t   at wing tip or pertaining to tip tank

v   pertaining to boom-mounted lifting surface or in the
             presence of the lifting surface

α due to angle of attack

δ due to aileron deflection

Λ referred to axes parallel and perpendicular to elastic axis

O   rigid wing ($q^* = \bar{q} = 0$)

Superscripts:

c   due to concentrated force and moment

P   due to concentrated normal force

R   due to concentrated pitching moment

δ due to aileron deflection

Matrices:

[ ]   square matrix

{ }   column matrix

⌊ ⌋   row matrix

⌊ ⌉   diagonal matrix

[1]   identity matrix

$\begin{bmatrix}1_t\end{bmatrix}$ matrix defined by equation (29)

[A]   aeroelastic matrix (equation (13a))

$\begin{bmatrix}\overline{A}\end{bmatrix}$ auxiliary aeroelastic matrix (equation (13b))

$\begin{bmatrix}A_R\end{bmatrix}$ aileron-reversal matrix (equations (21) and (32))

[B]   matrix defined by equation (28)

$\{h\}$, $\{\overline{h}\}$ matrices defined by equations (14) and (30)

[I],[II]   single and double integrating matrices from tip to root
                     (prime mark on symbol I or II designates an integrating
                     matrix for a function which goes to zero with infinite
                     slope at wing tip)

$[I]^{''}$ single integrating matrix from root to tip

$\lfloor I_1 \rfloor$, $\lfloor II_1 \rfloor$ first rows of matrices [I] and [II]

[Q]   matrix of aerodynamic influence coefficients

METHOD OF ANALYSIS

Matrix - Integration Method

Résumé of method of references 1 and 2.- The method of references 1
and 2 is based on numerical integrations of the equations of structural
equilibrium by means of suitable integrating matrices. These integrating
matrices, together with other matrices and constants which describe the
structural, aerodynamic, and geometric properties of the given wing, are
assembled into aeroelastic, auxiliary aeroelastic, and aileron-reversal
matrices, from which the structural twist at any dynamic pressure, as
well as the dynamic pressures required for divergence and reversal, can
be determined. The method of references 1 and 2 was modified slightly
in the following résumé.

The limitations of the method of references 1 and 2 are discussed
in those papers; they arise from the assumptions that the spanwise lift
and pitching-moment distributions can be predicted for any given angle-
of-attack distribution by means of the aerodynamic influence coeffi-
cients and that the structural deformations can be predicted by simple

beam theory plus rigid-body rotations imparted by the root. (In refer-
ences 1 and 2 a method is also presented for using structural influence
coefficients measured on the actual wing or calculated by methods more
refined than simple beam theory; this method can be extended to the
case of wings with concentrated forces at the tip in the same manner as
employed in the present paper for the method based on simple beam
theory.)

The loading coefficient $cc_l/\overline{c}$ for any section of the wing
parallel to the stream may be determined for any angle-of-attack dis-
tribution by means of suitable aerodynamic influence coefficients Q_s
and Q_a (for symmetric and antisymmetric lift-distributions, respec-
tively) in the form

$$\left\{\frac{cc_l}{\overline{c}}\right\} = C_{L_\alpha}\left[Q_a\right]\{\alpha\} + C_{l_d}\alpha_\delta\delta\left\{\frac{cc_l}{\overline{c}C_{l_d}}\right\}_\delta \tag{1}$$

where α is the total angle of attack at a given point on the span due
to geometrical setting and structural deformation, C_{L_α} is the rigid-
wing lift-curve slope, C_{l_d} is the negative of the coefficient of

damping in roll, and $\left\{\dfrac{cc_l}{\overline{c}C_{l_d}}\right\}_\delta$ is $\dfrac{1}{C_{l_d}}$ times the section loading coef-

ficient due to aileron deflection for a unit equivalent angle of
attack $\alpha_\delta\delta$; the matrix $\left[Q_a\right]$ is used for the sake of definiteness.
Approximate influence-coefficient matrices Q_s and Q_a may be calcu-
lated for subsonic flow by the method of reference 3. The lift on any
section can then be written as

$$\{l\} = q\overline{c}\left\{\frac{cc_l}{\overline{c}}\right\} \tag{2}$$

and the section pitching moment about the elastic axis in planes
parallel to the free stream can be written as

$$\{t\} = e_{1_r}\overline{c}\left\lfloor\frac{e_1}{e_{1_r}}\frac{c}{\overline{c}}\right\rceil\{l\}_\alpha - e_{1_r}\overline{c}\lfloor\epsilon\rceil\left\lfloor\frac{e_1}{e_{1_r}}\frac{c}{\overline{c}}\right\rceil\{l\}_\delta \tag{3}$$

where the subscripts α and δ serve to specify the lifts due to the
loading coefficients represented by the first and second term on the

right-hand side of equation (1), respectively, and where ϵ is the ratio of the moment arm e_2 to the moment arm e_1. (See fig. 1.) The parameter e_{1_r} is an arbitrary reference value of the dimensionless section moment arm e_1.

The section lift and section torque given by equations (2) and (3) can be integrated by means of integrating matrices to obtain the accumulated bending and twisting moments at any section about a pair of axes parallel and perpendicular to the free stream, respectively, with their origin at the elastic axis at that section. Thus,

$$\{M\} = \left(\frac{b'}{2}\right)^2 [II]\{l\} \tag{4}$$

$$\{T\} = \frac{b'}{2}[I]\{t\} - \tan \Lambda \{M\} \tag{5}$$

where the matrices $[I]$ and $[II]$ are defined and given in reference 1. If the lift distribution goes to zero with infinite slope at the wing tip, the matrices must be modified to take this fact into account; the resulting matrices are designated by $[I']$ and $[II']$, respectively.

The bending and twisting moments obtained in this manner can be transferred to axes along and perpendicular to the elastic axis; the resulting moments are

$$\{M_\Lambda\} = \cos \Lambda \{M\} - \sin \Lambda \{T\} \tag{6}$$

$$\{T_\Lambda\} = \sin \Lambda \{M\} + \cos \Lambda \{T\} \tag{7}$$

The structural twist φ and the slope of the structural-deformation curve Γ can then be obtained by an integration of the products T_Λ/GJ and M_Λ/EI, respectively. These integrations can be performed numerically by means of the matrix $[I]''$, which, for equally spaced stations, is the double transpose of the matrix $[I]$. Consequently,

$$\{\varphi\} = \frac{b'/2}{(GJ)_r \cos \Lambda}[I]'' \left\lfloor\frac{(GJ)_r}{GJ}\right\rfloor \{T_\Lambda\} \tag{8}$$

Error

An error occurred while processing this page. See the system log for more details.

$$\{h\} = [\bar{A}] \left\{ \frac{cc_l}{\bar{c}c_{l_d}} \right\}_\delta \tag{14}$$

$$k = \frac{(GJ)_r}{(EI)_r} \frac{b'/2}{e_{l_r}\bar{c}} \frac{\tan \Lambda}{\cos^2\Lambda} \tag{15}$$

$$\kappa = \frac{c_{l_d}}{c_{L_\alpha}} \tag{16}$$

and where α_δ is the effective angle of attack due to unit aileron deflection. If the rigid-wing, lift-curve slope C_{L_α} in equation (12) is based on a nonlinear lift curve, the value of C_{L_α} should be taken at an average angle-of-attack condition. For symmetric cases the matrix $[Q_s]$ is used instead of $[Q_a]$ in equation (13) and the second term on the right-hand side of equation (11) is disregarded; for lift distributions which go to zero with infinite slope at the tip, the matrices $[I']$ and $[II']$ are used in equations (13) and (14) instead of $[I]$ and $[II]$.

The aeroelastic equation (11) can be solved for α_s and for the dynamic pressure at divergence or reversal in the manner described in references 1 and 2. Specifically, the reversal speed can be obtained by determining the eigenvalues of a matrix $[A_R]$ obtained in the following manner: At reversal the rolling moment due to aileron deflection is to be zero, so that

$$C_{L_\alpha} q\bar{c}\left(\frac{b}{2}\right)^2 \left(\kappa\alpha_\delta\delta \lfloor II_0 \rfloor \left\{ \frac{cc_l}{\bar{c}c_{l_d}} \right\}_\delta + \lfloor II_0 \rfloor [Q_c] \{\alpha_s\} \right) = 0 \tag{17}$$

where

$$\lfloor II_0 \rfloor = \left(\frac{b'}{b}\right)^2 \lfloor II_1 \rfloor + \frac{w}{b}\frac{b'}{b} \lfloor I_1 \rfloor \tag{18}$$

and where, in turn, $\lfloor II_1 \rfloor$ and $\lfloor I_1 \rfloor$ are the first rows of the
matrices $[II]$ and $[I]$. Hence,

$$\alpha_\delta \delta = -\frac{\lfloor II_0 \rfloor [Q_a] \{\alpha_s\}}{\kappa \lfloor II_0 \rfloor \left\{\dfrac{cc_l}{\overline{c}c_{l_d}}\right\}_\delta} \tag{19}$$

so that, upon substitution of equation (19) into the second term on
the right-hand side of equation (11), this equation becomes

$$\{\alpha_s\} = q^* [A_R] \{\alpha_s\} \tag{20}$$

where the aileron-reversal matrix $[A_R]$ is defined by

$$[A_R] = [A] + \frac{1}{g} \{h\} \lfloor II_0 \rfloor [Q_a] \tag{21}$$

and

$$g = \kappa \lfloor II_0 \rfloor \left\{\frac{cc_l}{cc_{l_d}}\right\}_\delta \tag{22}$$

In the derivation of equation (20), the total angle of attack $\{\alpha\}$ has
been replaced by $\{a_s\}$ in equation (11) because the geometric angle
of attack has no effect on aileron reversal.

Modifications required for inclusion of tip forces.- As a result
of the fact that the method of references 1 and 2 uses the equation of
structural equilibrium in integral rather than in differential forms
the inclusion of concentrated tip forces is accomplished quite readily
by including additional matrices which introduce the effect of the con-
centrated forces at the tip in the aeroelastic and aileron-reversal
matrix. These matrices are then treated in the same manner as those
for the wing without concentrated forces. In essence this procedure
amounts to performing a separate analysis for the wing with and without

the concentrated forces, although many of the matrices calculated in
the wing-alone analysis can be used in the other analysis. This method
is subject to the same limitations as the method of references 1 and 2;
in particular, the aerodynamic forces on the wing must be predictable
by means of suitable influence coefficients.

If the normal force at the tip is P_t and has a pitching moment T_t
about the elastic axis in a plane parallel to the plane of symmetry,
equations (4) and (5) become

$$\{M\} = \left(\frac{b'}{2}\right)^2 [II]\{l\} + \frac{b'}{2}[1 - \eta^*]\{P_t\} \tag{23}$$

and

$$\{T\} = \frac{b'}{2}[I]\{t\} - \tan \Lambda \{M\} + \{T_t\} \tag{24}$$

The column matrices $\{P_t\}$ and $\{T_t\}$ consist of elements all equal
to P_t and T_t, respectively, and η^* is the dimensionless lateral
distance from the root to the station at which the bending and twisting
moments are obtained. If the concentrated force and moment are due to
aerodynamic action they may conveniently be expressed in terms of dimen-
sionless coefficients as

$$P_t = C_{L_{\alpha_t}} qS_t(\alpha_t + K\delta) \tag{25}$$

$$T_t = C_{L_{\alpha_t}} qdS_t(\alpha_t + K\delta) \tag{26a}$$

or

$$T_t = C_{m_{\alpha_t}} q\bar{V}_t(\alpha_t + K\delta) \tag{26b}$$

where α_t is the value of the total angle of attack at the tip and
where equation (26a) pertains to a boom-mounted lifting surface with a
center of pressure at a distance d ahead of the elastic axis, and
equation (26b) pertains to a tip tank with volume $\bar{V}_t$. For the sake of
definiteness equation (26a) is used in the following analysis. The
factor K in equations (25), (26a), and (26b) is the gear ratio between
the boom deflection and the aileron deflection. In the case of a tip

tank or in the case of a lifting surface which is not geared to the aileron, the factor K is zero.

When equations (4) and (5) are replaced by equations (23), (24), (25), and (26a), the aeroelastic equation (11) becomes

$$\{\alpha_s\} = q^*\left[[A] + [B]\left[1_t\right]\right]\{\alpha\} - q^*\alpha_\delta\delta\{\bar{h}\} \tag{27}$$

where

$$[B] = \frac{C_{L_{\alpha_t}}}{C_{L_\alpha}}\frac{S_t}{\bar{c}(b'/2)}[I]''\left[\frac{\bar{d}}{e_{1r}\bar{c}}\left[\left[\frac{(GJ)_r}{GJ}\right] + \frac{(GJ)_r}{(EI)_r}\tan^2\Lambda\left[\frac{(EI)_r}{EI}\right]\right] - \right.$$

$$\left. k\left[\frac{(EI)_r}{EI}\right]\left[1 - \eta^*\right]\right] \tag{28}$$

$$\left[1_t\right] = \begin{bmatrix} . & . & 0 & 0 & 0 & 1 \\ . & . & 0 & 0 & 0 & 1 \\ . & . & 0 & 0 & 0 & 1 \\ . & . & 0 & 0 & 0 & 1 \\ . & . & . & . & . & . \\ . & . & . & . & . & . \end{bmatrix} \tag{29}$$

$$\{\bar{h}\} = \{h\} - \frac{K}{\alpha_\delta}[B]\{1\} \tag{30}$$

and $\{1\}$ is a column all the elements of which are equal to 1.

The aeroelastic equation (27) can be solved in the same manner as equation (11) for $\{\alpha_s\}$ or for the dynamic pressure at divergence. An aileron-reversal matrix can be calculated in the manner employed to obtain equation (22). The rolling moment due to aileron deflection vanishes when

$$C_{L_\alpha} q\bar{c}\left(\frac{b}{2}\right)^2\left(\kappa\alpha_\delta\delta\lfloor II_0\rfloor \left\{\frac{cc_l}{\bar{c}c_{l_d}}\right\}_\delta + \lfloor II_0\rfloor[Q_a]\{\alpha_s\} + \right.$$

$$\left. \frac{C_{L_{\alpha_t}}}{C_{L_\alpha}}\frac{S_t}{\bar{c}(b/2)}K\delta + \frac{C_{L_{\alpha_t}}}{C_{L_\alpha}}\frac{S_t}{\bar{c}(b/2)}\lfloor l_t\rfloor\{\alpha_s\}\right) = 0 \qquad (31)$$

where the last two terms on the left-hand side represent the rolling moment of the lift on the boom-mounted lifting surface and where the matrix $\lfloor l_t\rfloor$ is the first row of the matrix $[l_t]$. If $\alpha_\delta\delta$ is obtained from equation (31) and substituted into equation (27) the resulting equation is identical in form with equation (21), except that the aileron-reversal matrix is replaced by a new matrix $[A_R]$

$$[A_R] = [A] + [B][l_t] + \frac{1}{g'}\{\bar{h}\}\left|\lfloor II_0\rfloor[Q_a] + \frac{C_{L_{\alpha_t}}}{C_{L_\alpha}}\frac{S_t}{\bar{c}(b/2)}\lfloor l_t\rfloor\right| \qquad (32)$$

where

$$g' = \kappa\lfloor II_0\rfloor\left\{\frac{cc_l}{\bar{c}c_{l_d}}\right\}_\delta + \frac{C_{L_{\alpha_t}}}{C_{L_\alpha}}\frac{S_t}{\bar{c}(b/2)}\frac{K}{\alpha_\delta} \qquad (33)$$

Simplified Method

The simplified method is applicable in cases for which the aerodynamic interaction between the wing proper and the source of the concentrated aerodynamic force at the wing tip is neglected. This method consists of determining the aeroelastic twist of a wing subjected to concentrated torques (or pitching moments) and normal forces of known magnitude applied at its tip at one dynamic pressure. This information is combined with the aerodynamic characteristics of a boom-mounted lifting surface, and the results are extrapolated over the range of dynamic pressures of interest on the basis of the semirigid-wing concept; the dynamic pressures at divergence and reversal are determined from this extrapolation.

This simplified method is subject to the same limitations and to two others, as well. The semirigid concept furnishes a useful basis for extrapolation of aeroelastic results only if the lowest root of the polynomial for the dynamic pressure at divergence is much lower in absolute value than the next higher one, as seems to be the case for actual wings. Also, as developed in this paper, aerodynamic interaction between the source of the concentrated force and the wing proper is not taken into account. If the magnitude of this interaction can be predicted it can be taken into account in the simplified method by certain modifications, as discussed in a later section, but in such a case it may be more expedient to use the other method presented in this paper.

The effect of concentrated forces of known magnitudes on the aeroelastic characteristics of a wing alone.- If a concentrated normal force P and a concentrated pitching moment R are applied to the wing tip, the bending and twisting moments about axes parallel and perpendicular to the plane of symmetry are

$$\{M\} = P \frac{b'}{2} \{1 - \eta^*\} \tag{34}$$

and

$$\{T\} = -\tan \Lambda \{M\} + R \{1\} \tag{35}$$

From these moments the angle-of-attack change $\alpha_s{}^c$ caused by these concentrated forces can then be calculated from equation (10) by using equations (6), (7), (8), and (9). The resulting expression for $\alpha_s{}^c$ may be written as

$$\{\alpha_s{}^c\} = R \left\{ \frac{\cos \Lambda (b'/2)}{(GJ)_r} [I]'' \left\lfloor \frac{(GJ)_r}{GJ} \right\rfloor \{1\} + \right.$$

$$\left. \frac{\sin^2\Lambda(b'/2)}{(EI)_r \cos \Lambda} [I]'' \left\lfloor \frac{(EI)_r}{EI} \right\rfloor \{1\} \right\} -$$

$$P \left\{ \frac{\tan \Lambda(b'/2)^2}{(EI)_r \cos \Lambda} [I]'' \left\lfloor \frac{(EI)_r}{EI} \right\rfloor \{1 - \eta^*\} \right\} \tag{36}$$

where $\alpha_s{}^c$ is the angle-of-attack change produced directly by the con-
centrated forces without the presence of aeroelastic effects. If the
concentrated forces are caused by a boom-mounted lifting surface and if
the aerodynamic-induction effect of the wing on the lifting surface can
be neglected, then

$$P = C_{L_{\alpha_v}} S_v q \left(\alpha_t + K\delta \right) \tag{37}$$

and

$$R = C_{L_{\alpha_v}} S_v q d \left(\alpha_t + K\delta \right) \tag{38}$$

where α_t is the angle of attack of the wing at the tip and includes
both the angle of attack due to airplane attitude and that due to
structural deformation. Substitution of equations (37) and (38) into
equation (36) yields an expression which may be reduced to

$$\left\{ \alpha_s{}^c \right\} = \left(\alpha_t + K\delta \right) q^* \left\{ K_R \left\{ \alpha^R \right\} - K_P \left\{ \alpha^P \right\} \right\} \tag{39}$$

where

$$K_P \equiv \frac{C_{L_{\alpha_v}}}{C_{L_\alpha}} \frac{S_v}{\bar{c} \frac{b'}{2}} k \tag{40}$$

$$K_R \equiv \frac{C_{L_{\alpha_v}}}{C_{L_\alpha}} \frac{S_v}{\bar{c} \frac{b'}{2}} \frac{d}{\bar{c} e_{1_r}} \tag{41}$$

$$\left\{ \alpha^P \right\} \equiv \left[I \right]'' \left[\frac{(EI)_r}{EI} \right] \left\{ 1 - \eta^* \right\} \tag{42}$$

$$\left\{\alpha^R\right\} \equiv [I]''\left\lfloor\left\lfloor\frac{(GJ)_r}{GJ}\right\rfloor + \frac{(GJ)_r}{(EI)_r}\tan^2\Lambda\left\lfloor\frac{(EI)_r}{EI}\right\rfloor\right\rfloor\{1\} \qquad (43)$$

or, if $\dfrac{GJ}{(GJ)_r} = \dfrac{EI}{(EI)_r}$ equation (43) reduces to

$$\left\{\alpha^R\right\} = \left(1 + \frac{(GJ)_r}{(EI)_r}\tan^2\Lambda\right)[I]''\left\lfloor\frac{(EI)_r}{EI}\right\rfloor\{1\} \qquad (44)$$

Aeroelastic effects on the angle-of-attack change due to concentrated forces.- The aeroelastic effects of the angle-of-attack change due to the concentrated forces given by equation (39) can be calculated by introducing this angle-of-attack change in the right-hand side of equation (11) provided that the aerodynamic-induction effects of the boom-mounted lifting surface on the wing are neglected. Hence

$$\left\{\alpha_s\right\} = q^*[A]\left\{\left\{\alpha_g\right\} + \left\{\alpha_s{}^c\right\} + \left\{\alpha_s\right\}\right\} - q^*\alpha_\delta\delta\left\{h\right\}$$

or

$$\left[[1] - q^*[A]\right]\left\{\alpha_s\right\} = q^*[A]\left\{\alpha_g\right\} + q^*[A]\left\{\alpha_s{}^c\right\} - q^*\alpha_\delta\delta\left\{h\right\} \qquad (45)$$

where $\left\{\alpha_s\right\}$ is the column which describes the angle-of-attack changes caused by aeroelastic action due to all three forcing loadings or angles of attack $\left\{\alpha_g\right\}$, $\left\{\alpha_s{}^c\right\}$, and $\left\{h\right\}$ and where, in turn, $\left\{\alpha_s{}^c\right\}$ can be considered to consist of two parts, as indicated in equation (39). The most convenient way of solving equation (45) consists of evaluating separately the contributions of $\left\{\alpha_g\right\}$, $\left\{\alpha^c\right\}$, and $\left\{h\right\}$. For this purpose equation (45) can be rewritten as

$$\Big[[1] - q^*[A]\Big] \{\bar{\alpha}_g\} = \{\alpha_g\} \tag{46}$$

$$\Big[[1] - q^*[A]\Big] \{\bar{\alpha}^P\} = \{\alpha^P\} \tag{47}$$

$$\Big[[1] - q^*[A]\Big] \{\bar{\alpha}^R\} = \{\alpha^R\} \tag{48}$$

$$\Big[[1] - q^*[A]\Big] \{\alpha_s{}^\delta\} = -\alpha_\delta \delta \{h\} \tag{49}$$

where $\bar{\alpha}_g$ is equal to α_g plus the part of α_s due to α_g and thus is the total (or net) angle of attack due to airplane attitude and the amount of aeroelastic deformation associated with that angle of attack at the given value of q^*; similarly $\bar{\alpha}^P$ and $\bar{\alpha}^R$ are equal to α^P and α^R plus the amount of aeroelastic deformation associated with these angle-of-attack distributions at the given value of q^*, and $\alpha_s{}^\delta$, when multiplied by q^*, is the amount of aeroelastic deformation associated with aileron deflection. In the matrix $[A]$ which occurs in equations (46), (47), and (48), $[Q_s]$ has to be used for symmetrical flight and $[Q_a]$ for antisymmetrical flight; in equation (49), $[Q_a]$ is used.

The total angle-of-attack distributions due to all forcing angle-of-attack distributions and their associated aeroelastic increments are then

$$\{\alpha\} = \{\bar{\alpha}_g\} + (\alpha_t + K\delta)q^*\left\{K_R\{\bar{\alpha}^R\} - K_P\{\bar{\alpha}^P\}\right\} + q^*\{\alpha_s{}^\delta\} \tag{50}$$

and hence, at the wing tip

$$\alpha_t = \bar{\alpha}_{g_t} + (\alpha_t + K\delta)q^*\left(K_R\bar{\alpha}_t{}^R - K_P\bar{\alpha}_t{}^P\right) + q^*\alpha_{s_t}{}^\delta \tag{51}$$

so that the angle of attack of the boom-mounted lifting surface is

$$\bar{\alpha}_t + K\delta = \frac{\bar{\alpha}_{g_t} + K\delta + q^*\alpha_{s_t}{}^\delta}{1 - q^*\left(K_R\bar{\alpha}_t{}^R - K_P\bar{\alpha}_t{}^P\right)} \tag{52}$$

The static aeroelastic analysis of a wing with a boom-mounted lifting surface at a given value of q^* may therefore be performed as follows: The columns $\left\{\bar{\alpha}_g\right\}$ and $\left\{\alpha_s{}^\delta\right\}$ are obtained as part of the analysis of the wing alone. For the vane, the parameters K_P and K_R as well as the columns $\left\{\alpha_s{}^P\right\}$ and $\left\{\alpha_s{}^R\right\}$ are calculated from equations (40), (41), (42), and (43). Hence, the columns $\left\{\bar{\alpha}^P\right\}$ and $\left\{\bar{\alpha}^R\right\}$ are obtained by solving equations (47) and (48), respectively. $\bigg($If Crout's method (reference 4) was used to obtain $\left\{\bar{\alpha}_g\right\}$ and $\left\{\alpha_s{}^\delta\right\}$, then the evaluation of the two new columns requires very little additional effort; if series-expansion or iteration method was used to calculate $\left\{\bar{\alpha}_g\right\}$ and $\left\{\alpha_s{}^\delta\right\}$, then a new iteration is required, which should converge more rapidly than that for $\left\{\bar{\alpha}_g\right\}$, since experience indicates that $\left\{\alpha^P\right\}$ and $\left\{\alpha^R\right\}$ tend to approximate the dominant modal column of the matrix $[A]$ more closely than does $\left\{\alpha_g\right\}.\bigg)$ The angle of attack of the lifting surface can then be determined from equation (52), hence, the new angle-of-attack distribution from equation (50) and, finally, the lift distribution from equation (1). The lift on the lifting surface itself can be obtained from equation (37).

Extrapolation of aeroelastic characteristics calculated for one value of q^* to other values of q^*.- The foregoing procedure can be repeated for any value of q^* of interest, but the values of q^*_D and q^*_R cannot be obtained directly from this analysis. In order to calculate these values and to permit the extrapolation of results calculated by the method indicated in the preceding paragraph, the semirigid-wing concept may be used provided that the lowest root of the polynomial for the dynamic pressure at divergence is much lower in absolute value than the next higher one. In essence, this concept consists of reducing the degrees of freedom inherent in the structural deformations of the wing

to two by stipulating shape of the bending and twisting deformations and calculating the magnitude of each.

For the purpose at hand, the results of a semirigid analysis can be obtained by considering a rigid constant-chord wing permitted to rotate about hinges at its root parallel and perpendicular to its leading edge subject to the restraint of a torsion and a bending spring with constants K_T and K_M, respectively. In this case, the lift on one half-wing is

$$\frac{L}{2} = C_{L_\alpha} q \frac{S}{2}(\alpha_g + \alpha_s)$$

The twisting moment about the torsion hinge is

$$T_\Lambda = e_1 c \cos \Lambda \frac{L}{2}$$

The bending moment about the bending hinge is

$$M_\Lambda = \overline{y}^* \frac{b/2}{\cos \Lambda} \frac{L}{2}$$

where $\overline{y}^*$ is the dimensionless lateral center of pressure. The angle of twisting deformation is

$$\varphi = K_T T_\Lambda$$

and the angle of bending deformation is

$$\Gamma = K_M M_\Lambda$$

so that the angle of attack due to structural deformation is

$$\alpha_s = \varphi \cos \Lambda - \Gamma \sin \Lambda$$

$$= q^*(1 - k)\left(\alpha_g + \alpha_s\right) \tag{53}$$

where the parameters q^* and k are similar to those previously defined but are defined in equation (53) as

$$q^* \equiv q K_T \cos^2 \Lambda C_{L_\alpha} e_1 c \frac{S}{2}$$

$$k \equiv \frac{M}{K_T} \frac{\tan \Lambda}{\cos^2 \Lambda} \frac{\overline{y}^*(b/2)}{e_1 c}$$

The solution of equation (53) can be expressed either as

$$\alpha_s = \frac{q^*(1 - k)}{1 - (1 - k)q^*} \alpha_g$$

or

$$\alpha = \frac{1}{1 - (1 - k)q^*} \alpha_g$$

where $\alpha = \alpha_g + \alpha_s$. Since divergence will occur when

$$q^*_D = \frac{1}{1 - k}$$

the preceding equations can be written as

$$\alpha_s = \frac{q^*/q^*_D}{1 - \dfrac{q^*}{q^*_D}} \alpha_g \tag{54}$$

and

$$\alpha = \frac{1}{1 - \frac{q^*}{q^*_D}} \alpha_g \tag{55}$$

As shown in reference 5, equation (54) yields a good approximation to the angle of structural deformation of an actual wing for all values of q^*, if a constant C obtained from an analysis for one value of q^* is introduced. This constant is different for each point along the span and for each geometric angle-of-attack condition. With this modification

$$\alpha_s = C \frac{q^*/q^*_D}{1 - \frac{q^*}{q^*_D}} \alpha_g \tag{56}$$

where q^* and q^*_D are now defined in accordance with equation (12) for the given wing. Hence,

$$\alpha = \frac{1 - (1 - C)\left(q^*/q^*_D\right)}{1 - \frac{q^*}{q^*_D}} \alpha_g \tag{57}$$

For the wing with a boom-mounted lifting surface the following approximate expressions can be written:

$$\bar{\alpha}_{g_t} = \frac{1 - \left(1 - C_1\right)\left(q^*/q^*_D\right)}{1 - \frac{q^*}{q^*_D}} \alpha_{g_t} \tag{58}$$

$$\bar{\alpha}_t{}^R = \frac{1 - \left(1 - C_2\right)\left(q^*/q^*_D\right)}{1 - \frac{q^*}{q^*_D}} \alpha_t{}^R \tag{59}$$

$$\bar{\alpha}_t{}^P = \frac{1 - (1 - C_3)(q^*/q^*{}_D)}{1 - \frac{q^*}{q^*{}_D}} \alpha_t{}^P \tag{60}$$

$$\bar{\alpha}_{s_t}{}^\delta = -\alpha_\delta \delta \; \frac{1 - (1 - C_4)(q^*/q^*{}_D)}{1 - \frac{q^*}{q^*{}_D}} h_t \tag{61}$$

where $q^*{}_D$ is the value at divergence of the parameter q^* defined by equation (12) for the wing alone and where h_t is the last element of the column $\{h\}$. By calculating $\bar{\alpha}_{g_t}$, $\bar{\alpha}_t{}^R$, $\bar{\alpha}_t{}^P$, and $\alpha_{s_t}{}^\delta$ at one value of q^* from equations (46), (47), (48), and (49), the constants C_1, C_2, C_3, and C_4 in equations (58), (59), (60), and (61) can be evaluated. These equations can then be substituted into equations (52) and (50) to yield, respectively,

$$\alpha_t + K\delta = \frac{1}{q^*} \frac{\left(1 - (1 - C_1)\frac{q^*}{q^*{}_D}\right)\alpha_{g_t} + \left(1 - \frac{q^*}{q^*{}_D}\right)K\delta - q^*\alpha_\delta\delta\left(1 - (1 - C_4)\frac{q^*}{q^*{}_D}\right)h_t}{\frac{1}{q^*} - \frac{1}{q^*{}_D} - K_R\alpha_t{}^R\left(1 - (1 - C_2)\frac{q^*}{q^*{}_D}\right) + K_P\alpha_t{}^P\left(1 - (1 - C_3)\frac{q^*}{q^*{}_D}\right)} \tag{62}$$

and

$$\{\alpha\} = \frac{1}{1 - \frac{q^*}{q^*{}_D}}\left\{\left[\lfloor 1 \rceil - \frac{q^*}{q^*{}_D}\lfloor 1 - C_1\rceil\right]\{\alpha_g\} - q^*\alpha_\delta\delta\left[\lfloor 1 \rceil - \frac{q^*}{q^*{}_D}\lfloor 1 - C_4\rceil\right]\{h\} + \right.$$

$$\left. q^*(\alpha_t + K\delta)\left\{K_R\left[\lfloor 1 \rceil - \frac{q^*}{q^*{}_D}\lfloor 1 - C_2\rceil\right]\{\alpha^R\} - K_P\left[\lfloor 1 \rceil - \frac{q^*}{q^*{}_D}\lfloor 1 - C_3\rceil\right]\{\alpha^P\}\right\}\right\} \tag{63}$$

Equation (62) gives the value of $\alpha_t + K\delta$ at any value of q^*.

Calculation of q^* at divergence and reversal.- The value of q^* at divergence of the wing with a boom-mounted lifting surface can be obtained by equating the denominator of the fraction on the right-hand side of equation (62) to zero. This procedure yields the quadratic equation

$$\left(\frac{1}{q^*_{D_V}}\right)^2 - \left(K_R\alpha_t{}^R - K_P\alpha_t{}^P + \frac{1}{q^*_D}\right)\frac{1}{q^*_{D_V}} +$$

$$\frac{1}{q^*_D}\left((1 - C_2)K_R\alpha_t{}^R - (1 - C_3)K_P\alpha_t{}^P\right) = 0 \qquad (64)$$

which can be solved for $1/q^*_{D_V}$ and, hence, for $q^*_{D_V}$, the value of q^* at divergence of the wing with a lifting surface. Of the two value of $q^*_{D_V}$ obtained in this manner, the smaller one in absolute magnitude is the critical one unless it corresponds to a negative value of q_{D_V}, in which case the larger is the critical one unless it also corresponds to a negative q_{D_V}, in which case the wing cannot diverge.

In order to calculate the reversal speed of the wing-with-lifting-surface combination, the sum of the rolling moments of the lift distribution due to structural twist and to aileron deflection and of the rolling moment caused by the lift on the boom-mounted lifting surface is set equal to zero, as in equation (31) which may be rewritten as follows:

$$\lfloor\Pi_0\rfloor\lbrack Q_a\rbrack\{\alpha\} + \kappa\alpha_\delta\delta\lfloor\Pi_0\rfloor\left\{\frac{cc_l}{\bar{c}c_{l_d}}\right\}_\delta + K_V(\alpha_t + K\delta) = 0 \qquad (65)$$

where

$$K_V = \frac{C_{L_{\alpha_V}}}{C_{L_\alpha}}\frac{S_V}{\bar{c}(b/2)} \qquad (66)$$

The value of $\{\alpha\}$ required in equation (65) can be obtained from equation (63). However, the effect of the approximations made in obtaining equation (63) can be minimized by first substituting equation (50) into equation (65) and then approximating the moments of the various lift distributions in the manner employed to approximate the angles of attack in equations (58) to (61). For the sake of convenience $\{\alpha\}$ may be calculated for $\alpha_\delta\delta = 1$ and $\alpha_\delta\delta$ set equal to 1 in equation (65); in the subsequent derivation this simplification is assumed to have been made. This procedure yields the equations

$$\lfloor II_0 \rfloor [Q_a] \left\{ \left(\alpha_t + \frac{K}{\alpha_\delta}\right)q^* \left\{ K_R \left\{\overline{\alpha}^R\right\} - K_P \left\{\overline{\alpha}^P\right\} \right\} + q^* \left\{\alpha_s\delta\right\} \right\} +$$

$$\kappa \lfloor II_0 \rfloor \left\{ \frac{cc_l}{\overline{c}C_{l_d}} \right\}_\delta + K_v\left(\alpha_t + \frac{K}{\alpha_\delta\delta}\right) = 0$$

or

$$\left(\alpha_t + \frac{K}{\alpha_\delta}\right)\left(q^* K_R K_2 \left(1 - (1 - C'_2)\frac{q^*}{q^*_D}\right) - q^* K_P K_3 \left(1 - (1 - C'_3)\frac{q^*}{q^*_D}\right) + \right.$$

$$\left. K_v\left(1 - \frac{q^*}{q^*_D}\right)\right) - q^* K_4\left(1 - (1 - C'_4)\frac{q^*}{q^*_D}\right) + \kappa K_0\left(1 - \frac{q^*}{q^*_D}\right) = 0 \qquad (67)$$

where K_0, K_2, K_3, K_4, C'_2, C'_3, and C'_4 are defined by the relations

$$\lfloor II_0 \rfloor \left\{ \frac{cc_l}{\overline{c}C_{l_d}} \right\}_\delta = K_0 \qquad (68)$$

$$\lfloor II_0 \rfloor [Q_a] \{\overline{\alpha}^R\} = K_2 \frac{1 - \left(1 - C'_2\right)\frac{q^*}{q^*_D}}{1 - \frac{q^*}{q^*_D}} \tag{69}$$

$$\lfloor II_0 \rfloor [Q_a] \{\overline{\alpha}^P\} = K_3 \frac{1 - \left(1 - C'_3\right)\frac{q^*}{q^*_D}}{1 - \frac{q^*}{q^*_D}} \tag{70}$$

$$\lfloor II_0 \rfloor [Q_a] \{\alpha_s\delta\} = -K_4 \frac{1 - \left(1 - C'_4\right)\frac{q^*}{q^*_D}}{1 - \frac{q^*}{q^*_D}} \tag{71}$$

The coefficients K_2, K_3, and K_4 are equal to the matrix products on the left-hand sides of equations (69), (70), and (71) with the columns $\{\alpha^R\}$, $\{\alpha^P\}$, and $\{h\}$ substituted for $\{\overline{\alpha}^R\}$, $\{\overline{\alpha}^P\}$, and $\{\alpha_s(\delta)\}$, respectively. The coefficients C'_2, C'_3, and C'_4 can then be obtained by evaluating the left-hand sides of equations (69), (70), and (71) with the columns obtained by solving equations (47), (48), and (49) at one value of q^* and substituting that same value of q^* and the previously calculated values of K_2, K_3, and K_4 on the right-hand sides of equations (69), (70), and (71).

The value of $\alpha_t + K/\alpha_\delta$ given by equation (62) can be substituted into equation (67) to yield

$$\left(\frac{1}{q^*_{R_v}}\left(\frac{1}{q^*_{R_v}} - \frac{1}{q^*_D}\right)\frac{K}{\alpha_\delta} - \left(\frac{1}{q^*_{R_v}} - \frac{1 - C_4}{q^*_D}\right)h_t\right)\left(K_R K_2\left(\frac{1}{q^*_{R_v}} - \frac{1 - C'_2}{q^*_D}\right) - K_P K_3\left(\frac{1}{q^*_{R_v}} - \frac{1 - C'_3}{q^*_D}\right) + \right.$$

$$\frac{K_v}{q^*_{R_v}}\left(\frac{1}{q^*_{R_v}} - \frac{1}{q^*_D}\right)\right) + \left(\frac{1}{q^*_{R_v}}\left(\frac{1}{q^*_{R_v}} - \frac{1}{q^*_D}\right) - K_R \alpha_t{}^R\left(\frac{1}{q^*_{R_v}} - \frac{1 - C_2}{q^*_D}\right) + \right.$$

$$\left. K_P \alpha_t{}^P\left(\frac{1}{q^*_{R_v}} - \frac{1 - C_3}{q^*_D}\right)\right)\left(\frac{\kappa K_0}{q^*_{R_v}}\left(\frac{1}{q^*_{R_v}} - \frac{1}{q^*_D}\right) - K_4\left(\frac{1}{q^*_{R_v}} - \frac{1 - C'_4}{q^*_D}\right)\right) = 0 \tag{72}$$

By collecting the terms of equal powers of $q^*_{R_V}$, equation (72) can be reduced to a fourth-degree polynominal in $q^*_{R_V}$. Of the four roots of this polynominal the lowest real one of appropriate sign (to correspond to a positive value of q) represents the critical aileron reversal speed.

Calculation of the effect of boom flexibility.- The effect of the bending flexibility of the boom on static aeroelastic phenomena can easily be taken into account in the method of the preceding sections. The flexibility of the boom may be defined by the angle-of-attack change of the lifting surface due to boom deformation per unit normal load applied at the lifting surface in still air K_B.

The change in angle of attack of the lifting surface due to boom flexibility is then, as a result of equation (37),

$$\Delta\alpha_t = PK_B$$

$$= C_{L_{\alpha_V}} S_V q K_B \left(\alpha_t + K\delta + \Delta\alpha_t \right) \tag{73}$$

or

$$\alpha_t + K\delta + \Delta\alpha_t = \frac{1}{1 - \dfrac{q^*}{q^*_{BD}}} \left(\alpha_t + K\delta \right) \tag{74}$$

where q^*_{BD} is the value of q^* required for divergence of the lifting surface as a result of boom flexibility, that is, considering the wing rigid. The value of q^*_{BD} is given by

$$q^*_{BD} = \frac{d \dfrac{b'}{2} \cos \Lambda}{K_B K_R (GJ)_r} \tag{75}$$

Equation (74) indicates that in order to take boom flexibility into account the angle of attack of the lifting surface $\alpha_t + K\delta$ must be

replaced by the product of this angle and the factor $\dfrac{1}{1 - \dfrac{q^*}{q^*_{BD}}}$. This

procedure is equivalent to multiplying either the lift-curve slope or the area of the lifting surface by this factor. Consequently, equations (50), (52), (62), and (63) are valid for the flexible-boom case provided the factors K_P and K_R in these equations are divided by the

factor $1 - \dfrac{q^*}{q^*_{BD}}$. The angle of attack of the lifting surface relative

to the free stream can be obtained by dividing the values given by equations (52) and (62) by this factor. The dynamic pressure at divergence can be obtained from equation (64) if the term $1/q^*_{BD}$ is added to the

three terms within the second parentheses and to the two terms within the third parentheses on the left-hand side of that equation. Similarly, the dynamic pressure at reversal can be obtained from equation (72) if

the term $\dfrac{1}{q^*_{R_V}}\left(\dfrac{1}{q^*_{R_V}} - \dfrac{1}{q^*_D}\right)$ underlined in equation (72) is multiplied by

the factor $q^*_{R_V}\left(\dfrac{1}{q^*_{R_V}} - \dfrac{1}{q^*_{BD}}\right)$.

The procedure outlined in this section can also be used to take into account the effect on static aeroelastic phenomena of the flexibility of the lifting surface itself by calculating the value of q^* required to diverge the lifting surface and using this value instead of q^*_{BD}.

Comparison of the Two Methods of Computation

A comparison of the numerical results of the two methods may be had from the following tabulation of some of the results for the case of the wing - lifting-surface combination at subsonic speeds with $K_V = 0.02$, $\dfrac{d}{c_t} = 1.5$, gear ratio 1, and an infinitely stiff boom discussed in a subsequent section of this paper:

Method	q^*_D	q^*_R(3)
Matrix-integration	-0.1692	1.368
Simplified	-.1699	1.375

In this tabulation $q*_R(3)$ is the third root (in absolute magnitude) of the polynomial for $q*_R$; the lowest two roots are complex conjugate numbers and, hence, have no physical significance. There is good agreement between the results of the two methods.

In view of the satisfactory agreement of the results of the two methods and in view of the fact that the simplified method is generally less time consuming than the matrix-integration method, the simplified method appears to be preferable in all cases where it is applicable, particularly when wing-alone calculations have been made previously or when a number of configurations involving different tip forces are to be analyzed for the same basic wing. The matrix-integration method is more widely applicable than the simplified method; when the simplified method is applicable the matrix-integration method is preferable only in the case where the source of the concentrated load is permanently installed, so that no wing-alone calculations need be made.

The extension of the two methods presented herein to the calculation of the aeroelastic effects of concentrated forces located at points on the span other than the tip presents a problem in that such a force gives rise to moment and torque distributions which are either discontinuous or have a discontinuous slope. Such distributions cannot generally be integrated accurately by the simple numerical methods on which the integrating matrices used in this paper are based. However, special integrating matrices which take these discontinuities into account can be set up for the purpose of calculating the structural deformation for any concentrated force or moment at a given point on the span. Also, interpolating matrices can be devised for calculating the angle of attack at a given point on the span in terms of the angle of attack at the points on the span used in the aeroelastic analysis. By incorporating these interpolating and special integrating matrices in the method of references 1 and 2 in a manner similar to that indicated for tip forces in the present paper, a method can be obtained for taking concentrated aerodynamic forces at points other than the tip into account in aeroelastic calculations.

SCOPE OF THE ILLUSTRATIVE CALCULATIONS

Unswept Wing with Tip Tank

The matrix-integration method presented in the preceding section has been used to calculate some static aeroelastic characteristics of an unswept wing with a tip tank. The geometric and some of the structural and aerodynamic characteristics pertinent to the aeroelastic

analysis as well as a plan form of the tip tank are given in table 1(a).
The wing plan form and the tank are the same as those used in reference 6, and some of the aerodynamic data used in the present paper have
been obtained from that reference; the wing lift and moment coefficients
are those for the wing with section B with and without the tank with
sealed gap at a Mach number of 0.8. The tank lift and moment coefficient
(referred to the mean aerodynamic chord and one-half the wing area) are
for the tank on the wing with section A and gap open, since these data
are not available for section B and gap closed. The lift-curve slope
and the moment-curve slope given in table 1(a) for the tank-on configuration are those for the wing alone in the presence of the tank; they
have been obtained by subtracting the lift and moment on the tank from
the total lift and moment on the wing-tank combination.

The stiffness distributions $EI/(EI)_r$ and $GJ/(GJ)_r$ of this wing
are assumed to be identical and are given by the dashed-line curve in
figure 2. They were obtained by means of the constant-stress concept
of reference 5 for the inner 70 percent of the semispan; in the outboard
30 percent of the semispan they are assumed to vary as the fourth power
of the chord.

The rigid-wing spanwise lift distributions of the wing alone, for
uniform angle of attack, for linear antisymmetric twist and due to
aileron deflection were obtained by the method of reference 7 and are
given in figure 3 by the lines labeled $q* = 0$. The spanwise lift
distribution for the wing with the tank at a uniform angle of attack was
estimated by distributing the additional lift carried by the wing due to
the presence of the tank near the tip; the resulting distribution over
the part of the wing not blanketed by the tank is shown in figure 3(a).
The rigid-wing lift distributions for the other two angle-of-attack conditions were then estimated by using the method of reference 3 in conjunction with the lift distribution for uniform angle of attack estimated
in this manner. The factors k_1, k_2, k_3, and k_4 required in the
method of reference 3 were obtained from the figures of reference 3 for
the aspect ratio which a wing without a tank would have to have in order
to have the same lift-curve slope as the actual wing in the presence of
the tank. The rigid-wing lift distributions for the part of the wing
not covered by the tank calculated in this manner are shown in figures 3(b) and 3(c) by the lines labeled $q* = 0$. Aerodynamic influence
coefficients for this wing were calculated by the method of reference 3
using the lift distributions shown in figures 3(a) and 3(b).

The spanwise variation of the local aerodynamic-center positions
of the wing alone was estimated from an analysis of lifting-surface
calculations and experimentally obtained pressure distributions on
similar wings and was adjusted to correspond to the pitching moment
measured in reference 6. This variation was modified slightly for the

tank-on configuration by using the assumed spanwise variation of the
additional lift carried by the wing due to the presence of the tank as
well as the assumed chordwise location of this increment in lift obtained
on the basis of the pitching-moment data of reference 6. The spanwise
variation of the moment arm e_1, which is the difference between the

local aerodynamic-center and elastic-axis locations, is shown in fig-
ure 4(a). The reference value of e_{1_r} was taken as the value

of $C_{m_\alpha}/C_{L_\alpha}$ for the wing alone.

The local centers of pressure due to aileron deflection were
obtained from the assumed section center of pressure due to aileron
deflection (42 percent chord), the local aerodynamic-center positions,
and the spanwise lift distributions due to aileron deflection by the
method outlined in reference 2. The dimensionless distances e_2 of the
centers of pressure due to aileron deflection from the elastic axis (see
(fig. 1) are also given in figure 4(a).

In the aeroelastic calculations the wing was assumed to be mounted
on a reflection plate, as in the tests of reference 6, so that $b' = b$.
The small angle of sweepforward of the elastic axis (1.6°) was neglected.
All root-rotation constants (see reference 1) were assumed to be zero.

Calculated for wing with tank on and off were the dynamic pressure
at divergence and the dynamic pressure at reversal; also calculated for
several values of q/q_D were the spanwise lift distributions due to

uniform angle of attack, due to linear antisymmetric twist, and due to
aileron deflections, the lift-curve slopes, the coefficients of damping
in roll, the rolling-moment coefficients due to aileron deflection, the
spanwise centers of pressure, and the rolling velocity per unit aileron
deflection.

Sweptback Wing with Boom-Mounted Lifting Surface

The geometric characteristics, as well as some of the assumed aero-
dynamic and structural characteristics of a 45° sweptback wing, for
which aeroelastic calculations similar to those described in the pre-
ceding section have been performed, are presented in table 1(b). The
stiffness distributions have been estimated in the same manner as that
employed for the unswept wing and are presented in figure 2. The rigid-
wing spanwise lift distributions at subsonic speeds were calculated by
the method of reference 7 and are shown in figure 5 by the lines
labeled $q^* = 0$. Aerodynamic influence coefficients for subsonic speeds
were calculated by the method of reference 3. For supersonic speeds
strip theory was used; the resulting lift distributions are shown in

figure 6. The moment arms e_1 and e_2 for subsonic speeds were esti-
mated in the manner employed for the unswept wing and are shown in fig-
ure 4(b); for supersonic speeds the values were estimated from linearized
two-dimensional theory. Reference values for e_{1_r} of 0.2 and 0 were
used arbitrarily in the calculations for subsonic and supersonic speeds,
respectively.

As in the case of the unswept wing the sweptback wing is considered
to be mounted on a reflection plate, and all root-rotation constants are
assumed to be zero. The aerodynamic interaction between wing and boom-
mounted lifting surface has been neglected in the calculations.

No specific boom-mounted-lifting-surface plan forms have been con-
sidered; the surfaces are characterized in the calculations by the area
ratio

$$K_v = \frac{C_{L_{\alpha_v}}}{C_{L_\alpha}} \frac{S_v}{S/2}$$

by the moment-arm ratio d/c_t, by the gear ratio K of lifting-surface
motion to aileron motion, and by the boom flexibility K_B or the dimen-
sionless dynamic pressure for boom divergence q^*_{BD} defined in equa-
tion (75). Calculations have been made for the combinations of these
parameters shown in table 2. The combinations for which $\frac{d}{c_t} = 0$ have
no physical significance and are used only to illustrate certain trends.

For each of these combinations the aeroelastic information listed
at the end of the preceding section was calculated using the simplified
method; for most of the combinations, excluding those with flexible
booms, calculations were also made by the matrix-integration method.
For a configuration with $K_v = 0.02$ and $\frac{d}{c_t} = 1.5$ calculations have
been made for an ungeared lifting surface (case 3) as well as for a
geared lifting surface with gear ratio $K = 1$ (case 4); the calcula-
tions for all other cases have been made only for a gear ratio of 1.

RESULTS AND DISCUSSION

Unswept Wing with Tip Tank

The lift distributions of the unswept wing with and without tip tank for the three angle-of-attack conditions considered are shown in figure 3 at several values of $q*$. The values of $q*$ for the wing with the tank are based on the value of C_{L_α} for the wing without the tank, so that for the same value of $q*$ the dynamic pressures for the wing with and without the tip tank are the same, since all other quantities that enter into the definition of $q*$ are the same for both cases.

The effect of aeroelastic action is, as expected, to increase the lift at all points on the span, particularly in the region near the tip. This increase is much more pronounced for the wing with tip tank than for the wing without tip tank; even at somewhat lower values of the dynamic pressures ($q* = 0.192$ as opposed to $q* = 0.255$) the increase in lift on the wing with the tip tank is much greater than that on the wing without the tip tank. These two values of $q*$ represent the same fraction of $q*_R$ and differ from each other because $q*_R$ is different for the two cases.

The wing lift coefficient, lateral center of pressure, rolling-moment coefficient, and rate of roll obtained by integrating the lift distributions shown in figure 3 are presented in figure 7 as functions of the dimensionless dynamic pressure $q*$ (referred to the value of C_{L_α} for the wing without tip tank, as in figure 3). The lift is seen to increase much more rapidly for the wing with the tip tank than for the wing without the tip tank; the spanwise center of pressure is farther outboard at $q* = 0$ and moves outboard more rapidly with increasing $q*$ for the wing with the tip tank than for the wing without the tip tank.

At $q* = 0$ (rigid wing) the rolling-moment coefficient due to unit aileron deflection is 0.220 for the wing without tip tank and 0.291 for the wing with tip tank; for the wing without tip tank it decreases with increasing $q*$, whereas for the wing with tip tank it increases with increasing $q*$. The coefficient of damping in roll is 0.436 for the wing without tip tank and 0.685 for the wing with tip tank; it increases with increasing $q*$ in both cases but much more rapidly in the case of the wing with tip tank. The rate of roll is less at $q* = 0$ for the wing with tip tank than for the wing without tip tank and decreases more rapidly with increasing $q*$.

The value of $q*$ required to diverge the wing without tip tank is 1.021, and the value for the wing with tip tank is 0.380; the value

of $q*$ required to reverse the lateral control of the wing without tip tank is 0.819, whereas for the wing with tip tank the reversal speed is higher than the divergence speed, the value of $q*_R$ being 0.409. (The value of $q*$ for antisymmetric divergence of the wing with tip tank is 0.388.)

As may be seen from the results presented in the preceding para-graphs, the tip tank tends to have a very unfavorable effect on the static aeroelastic characteristics of the wing; for instance, the dynamic pressure required to diverge the unswept wing with the tip tank considered in this paper is very much lower than that required to diverge the wing alone. This is due in part to the higher lift carried by the wing and the more forward local aerodynamic centers, particularly near the tip, that result from the presence of the tank and in part to the concentrated moment introduced by the tank proper. Consequently, a wing which does not diverge by itself may diverge in the presence of the tip tank. Actually, the wing may destroy itself even before reaching the lowered divergence speed, because as it approaches this speed, the lateral center of pressure moves so far outboard and the lift-curve slope becomes so large that a relatively small gust may overstress the wing.

The values given here for the decrease in dynamic pressure required for divergence and increase in severity of the static aeroelastic phenomena, in general, may be somewhat pessimistic for two reasons. The stiffness distribution assumed for the wing is likely to be too low near the tip compared to actual airplanes. A somewhat higher stiffness near the tip would tend to reduce the severity of the aeroelastic effects greatly, since these effects tend to be quite sensitive to the stiffness near the tip. Also the combination of the aerodynamic data used in the calculations may not be realized on an actual wing. The lift on the wing-tank combination was taken for section B (reference 6) with and without a tank with sealed gap, but the lift on the tank was obtained for the tank on the model with section A and gap open, because no data were available for the lift on the tank on a model with section B and gap sealed. Also, the use of fins on the tip tank to overcome its inherent pitching moment would tend to reduce the severity of the static aeroelastic phenomena.

The lateral-control power of the wing-tank combination exhibits two interesting features. The aileron reversal speed of the wing with the tank is slightly higher than the antisymmetric divergence speed, and the rolling moment due to aileron deflection increases with dynamic pres-sure. Figure 7(b) of reference 2 indicates that the dynamic pressures required to reverse the lateral control of an unswept wing is propor-tional to the reciprocal of the sum of the moment arms e_1 and e_2. If e_2 is zero the reversal and divergence speeds coincide, and if e_2 is negative; that is, if the center of pressure due to aileron deflection

is forward of the elastic axis, the reversal speed is higher than the
divergence speed because the lift due to aileron deflection tends to
increase the angle of attack. The aileron reversal speed has no
physical meaning in such a case. As shown in figure 4 of the present
paper the assumed value of e_2 is negative over most of the span in
the case of the wing with the tip tank; in the case of the wing without
the tip tank, it is positive at the tip region, which is instrumental
in determining the aeroelastic characteristics of a wing. For the same
reason the rolling moment due to aileron deflection increases with
dynamic pressure in the case of the wing with a tip tank but decreases
in the case of the wing without a tip tank.

No dynamic effects have been considered in the analysis of this
paper, so that nothing qualitative may be said concerning the flutter
characteristics of the wing with the tip tank nor its dynamic-response
characteristics in abrupt maneuver. However, there is reason to believe
the wing with tip tank may well be subject to unfavorable dynamic
phenomena for some conditions of fuel mass in the tank at dynamic pres-
sures even lower than these at which static aeroelastic phenomena become
important.

Certain quasi-steady dynamic phenomena can be estimated by means of
the semirigid concept outlined in a preceding section, for instance, the
effect of inertia in a pull-out at constant load factor. As long as the
center of gravity is ahead of the elastic axis the effect of inertia is
to relieve the static aeroelastic phenomena. Since the inertia forces
are related to the normal acceleration which, in turn, is related to the
lift, there is a definite relation between the inertia and aerodynamic
forces. If the assumption is made that the tail and the fuselage carry
no lift, then the dynamic pressure at dynamic divergence - that is, at
divergence under conditions which permit the airplane as a whole to
accelerate in a direction normal to the flight path - can be estimated
by multiplying the static divergence speed by the factor

$$\frac{1}{1 - \dfrac{d_m}{e_{1_r}\bar{c}}\dfrac{Mg}{W}}$$

where d_m is the distance of the center of gravity of the wing plus tip
tank ahead of the elastic axis of the wing, M the mass of the wing plus
that of the two tip tanks, and W/g the mass of the airplane including
that of the wing and of the two tip tanks. $\left(\text{For } \dfrac{d_m}{e_{1_r}\bar{c}}\dfrac{Mg}{W} > 0.2 \text{ this}\right.$
correction tends to yield values of q_D which are somewhat too high.$\Big)$
Quasi-static dynamic effects can then be included approximately in the
static aeroelastic results presented in figures 3 and 7 by using the
value of q^*_D corrected in this manner in the ratio q^*/q^*_D used as

a parameter and the abscissa, respectively, in these two figures. A similar but more complicated correction factor which takes into account the lifts on the tail and fuselage may be devised.

Swept Wing With Boom-Mounted Lifting Surface

The spanwise lift distribution corresponding to three angle-of-attack conditions of the swept wing with and without two boom-mounted lifting-surface configurations are shown in figure 5 for subsonic speeds and for dimensionless dynamic pressures $q*$ of 0 and 0.169. Similarly, the spanwise lift distributions of the swept wing with and without one lifting-surface configuration are shown in figure 6 for supersonic speeds and for dimensionless dynamic pressures $\overline{q}$ of 0 and 2.17. In both figures 5 and 6 the lifting surfaces are considered to be mounted on a rigid boom and geared to the aileron with a gear ratio of 1. The dimensionless dynamic pressures of $q* = 0.169$ and $\overline{q} = 2.17$ both represent the negatives of the dynamic pressures which would diverge the wing without a lifting surface at subsonic and supersonic speeds, respectively. The dimensionless dynamic pressure $\overline{q}$ is used for the supersonic case because e_{1_r} was taken as 0 for that case, so that $q*$ is 0 regardless of q. The antisymmetric lift distributions are plotted in the form $cc_l/\overline{c}C_{l_d}$, which is similar to the form $cc_l/\overline{c}C_{L_\alpha}$ used for the symmetrical cases; the coefficient C_{l_d} is the negative of the conventionally defined coefficient of damping in roll.

As may be expected, the aeroelastic effect on the spanwise lift distributions is very large at the relatively high dynamic pressures represented in figures 5 and 6. The effect of the boom-mounted lifting surfaces, however, is almost negligible except near the wing tip and except in the case of the lift distribution due to aileron deflection.

The lift coefficients, aerodynamic-center locations, rolling-moment coefficients, and wing-tip helix angles obtained by integrating the lift distributions shown in figures 5 and 6 are represented in figures 8 and 9. As indicated in figure 8 for subsonic speeds, the effect of the lifting surface on the lift coefficient is negligible up to the highest dynamic pressures likely to be of interest, that is, for values of $q*$ between 0.2 and 0.3. The effect of the lifting surface with $\frac{d}{c_t} = 1.5$ on the aerodynamic-center shift is negligible, but the lifting surface with $\frac{d}{c_t} = 2.0$ does have a favorable effect on the aerodynamic-center shift; for $q* = 0.2$ the aerodynamic-center shift due to aeroelastic action is 0.17 for the wing without a lifting surface and for

the wing with the lifting surface with $\frac{d}{c_t} = 1.5$ but is only 0.14 for

the wing with the lifting surface with $\frac{d}{c_t} = 2.0$.

For the particular sweptback wing under consideration the rolling-moment coefficient due to aileron deflection is substantially increased by the boom-mounted lifting surfaces at the highest dynamic pressures of interest. At $q^* = 0.2$, for instance, the rolling-moment coefficient is increased about 50 percent by the lifting surface with $\frac{d}{c_t} = 1.5$ and about 100 percent by the lifting surface with $\frac{d}{c_t} = 2.0$. These increases are reflected in similar increases in the wing-tip helix angle per unit aileron deflection.

At dynamic pressures much higher than that corresponding to $q^* = 0.2$, the wings with lifting surfaces may diverge if the values of q^* given in table 2 are approached. For the wing without a lifting surface the smallest value of q^*_D is negative ($q^* = -0.169$), and the next larger one is also negative so that divergence is impossible. As may be deduced from figures 5, 6, 8, and 9 the divergence of the wings with lifting surfaces is a very localized phenomenon, affecting only the region of the wing near the tip. The aileron reversal speed of the wing with lifting surfaces tends to be much higher than that of the wing without lifting surfaces. (See table 2.)

As shown in figure 9, the effects of boom-mounted lifting surfaces on the aeroelastic behavior of this sweptback wing at supersonic speeds are very similar to the effects at subsonic speeds. The effects on the lift coefficient and aerodynamic-center shift are very small for the lifting surface with $\frac{d}{c_t} = 1.5$, but the rolling-moment coefficient and the wing-tip helix due to unit aileron deflection are increased considerably. The divergence speed of the wing with lifting surface is so high as to be of no practical interest, but the aileron reversal speed is relatively lower, compared to that of the wing without lifting surface, than in the subsonic case.

The lateral-control characteristics shown in figures 5, 6, 8, and 9 are for surfaces geared to the aileron with a 1:1 ratio. When the surface is not geared to the aileron the lift-curve slope, aerodynamic-center location, coefficient of damping in roll, and divergence speed are the same as when it is geared. The rolling moment and wing-tip helix angle due to aileron deflection as well as the reversal speed are even lower, however, for the ungeared surface than they are for the wing without a lifting surface, for instance, at subsonic speeds $C_{l_\delta}/C_{l_{\delta_0}}$

at $q* = 0.169$ is 0.261, 0.169, and 0.338 for the wing without a lifting surface, with ungeared surface, and with geared surface respectively; similarly, at supersonic speeds $C_{l_\delta}/C_{l_{\delta_0}}$ at $\overline{q} = 2.17$ is 0.276, 0.207, and 0.430, respectively, for these three cases. The values of $q*$ and $\overline{q}$ for reversal given in table 2 corroborate this trend. Inasmuch as an ungeared surface does not greatly improve the stability characteristics (aerodynamic-center shift) and is responsible for a deterioration of the lateral-control characteristics it will not be considered any further. In the following discussion the lifting surface will be assumed to be geared to the aileron, the gear ratio being 1:1 not because this is necessarily the optimum value but because that is the value for which the calculations described in this paper have been made.

The results presented so far for the sweptback wing with lifting surfaces have been for surfaces with an area ratio $K_V = 0.02$ mounted on idealized rigid booms. The effects of changes in lifting-surface area (or lift-curve slope) and in boom flexibility are shown in figure 10 for subsonic speeds. This figure shows that in order to decrease the aerodynamic-center shift due to aeroelastic action below that of the wing without a lifting surface a moment-arm ratio d/c_t of 1.5 or more is required regardless of the area of the surface, unless the boom is quite flexible. An increase in the moment-arm ratio from 1.5 to 2 or a decrease in the boom stiffness from infinite rigidity to a value of $q*_{BD}$ of about 0.4 serves to decrease the aerodynamic-center shift more than a doubling of the surface area (from $K_V = 0.02$ to $K_V = 0.04$).

Figure 10 also shows that an increase of about 40 percent may be had in the wing-tip helix angle due to unit aileron deflection of the wing alone by adding a lifting surface with $K_V = 0.02$ and $\frac{d}{c_t} = 1.5$ on a rigid boom. By increasing the area ratio to $K_V = 0.04$ or by reducing the rigidity of the boom until $q*_{BD}$ is about 0.4 an additional 60-percent increase may be had, but by increasing the moment-arm ratio of the lifting surface from $\frac{d}{c_t} = 1.5$ to $\frac{d}{c_t} = 2.0$ only an additional 30-percent increase is obtained.

The dimensionless dynamic pressures required for divergence and reversal of the wing-with-lifting-surface combinations represented in figure 10 are given in table 2. For the combinations with large moment arm, surface area, or with very flexible booms, divergence of the local type mentioned previously is likely to occur at relatively low dynamic pressures, in some instances so low as to be of practical concern. The reversal speed of all configurations is far too high to be of interest.

The effectiveness of a boom-mounted lifting surface as an aeroelastic-effect relieving device is probably best illustrated by figure 10. For the case considered in figure 10, that is, the swept-back wing flying at subsonic speeds with a value of $q*$ of 0.1687, the aerodynamic center is shifted 15 percent rearward from the rigid-wing position. As shown in figure 10 for a lifting surface with an effective area ratio K_v of 0.02, a moment-arm ratio d/c_t of 1.5, and a flexible boom with $q*_{BD}$ equal to 1/3 (which is twice the value of $q*$ considered in the figure) this shift is reduced to 10 percent. Larger values of K_v and d/c_t and lower values of $q*_{BD}$ are likely to be impractical because of dynamic (primarily flutter), mechanical, and weight considerations. In varying these three lifting-surface parameters it appears that more benefit may be had by varying the moment-arm ratio than by varying the area ratio a corresponding amount but that unless the moment-arm ratio is larger than about 1.5 no improvement in the shift of the aerodynamic center is had at all. A substantial improvement in the shift of the aerodynamic center can be obtained by increasing the flexibility of the boom, but too flexible a boom can lead to localized divergence of the wing, as well as to divergence of the boom proper; as shown in table 2 the wing diverges when $q*$ is 0.277 and 0.217 in the case of the lifting surface with $K_v = 0.02$, $\frac{d}{c_t} = 1.5$, and $q*_{BD}$ equal to 1/2 and 1/3, respectively. The use of a flexible boom is also likely to introduce flutter problems.

Figure 10 indicates that the lateral-control power and maneuverability characteristics may also be improved substantially by a geared lifting surface; by using a lifting surface with gear ratio $K = 1$, $K_v = 0.02$, $\frac{d}{c_t} = 1.5$, and $q*_{BD} = \frac{1}{3}$, the wing-tip helix angle is twice that of the wing without a lifting surface. Again, a variation in the moment-arm ratio appears to be more effective than a proportional increase in the area ratio but, again, a minimum value of $\frac{d}{c_t}$ $\left(\text{about } \frac{1}{2}\right.$ in this case$\left.\right)$ is required to obtain any improvement at all. In general, the improvement in the lateral-control characteristics obtainable by means of a boom-mounted lifting surface appears to be larger than the improvement in the shift of the aerodynamic center.

In evaluating the results discussed in the preceding paragraphs several facts must be kept in mind. Concerning the specific calculations described in this paper, as pointed out in connection with the calculations for the tip tank, the assumed wing stiffnesses may be relatively too low near the tip compared with actual practice, so that the magnitude of the various static aeroelastic effects may be overestimated somewhat in these calculations.

Furthermore, in the calculations for the boom-mounted lifting surface the effects of the upwash of the wing on the lift of the surface and of the downwash of the surface on the lift of the wing tip have been neglected. In the case of a rigid boom the effects of the upwash of the wing on the lift of the surface can be taken into account by multiplying the lift-curve slope of the lifting surface by a factor η_v which is one plus the value of the upwash angle per unit angle of attack of the wing tip. The upwash angle can be calculated by means of the charts of reference 8. Similarly, in the case of a rigid boom, the effect of the downwash of the lifting surface on the lift of the wing tip can be taken into account by calculating a factor η_W which is equal to one minus the downwash caused by the surface on the three-quarter-chord line of the wing at the wing tip; again, the charts of reference 8 can be used to calculate this downwash angle, if desired. The elements in the last column of the aerodynamic-influence-coefficient matrix $[Q]$ are then multiplied by this factor. In the case of a flexible boom the method of analysis presented in this paper must be modified slightly; for instance, the angle of attack of the lifting surface is then equal to the angle of boom deformation plus the product of the angle of attack of the wing tip and the aforementioned factor η_v.

Finally, no dynamic effects have been taken into account in the calculations, nor can a simple correction be given for quasi-static dynamic effects. However, qualitatively the quasi-static dynamic effects are adverse, inasmuch as they decrease the normal force available from the lifting surface. The essentially dynamic phenomena, such as encountered in flutter, gusts, or abrupt maneuvers are also likely to be affected adversely by boom-mounted lifting surfaces, particularly by heavy surfaces with long or flexible booms. In general, all means of improving static aeroelastic characteristics by balancing the effects of bending and twisting deformations, rather than by stiffening the structure, have certain difficulties in common. Exact balance is difficult to achieve, and if it is achieved for one Mach number it may not hold at others; certainly a condition of balance obtained at subsonic speeds is unlikely to carry over to supersonic speeds. Nor does such a means of improving static aeroelastic characteristics necessarily improve dynamic characteristics; in fact, more often than not, it effects the dynamic characteristics adversely.

As a result of these considerations no optimum boom-mounted lifting-surface configuration can be selected. Such a configuration depends on the magnitude and nature of the aeroelastic effects that must be alleviated and the weight penalty that can be tolerated in order to achieve this alleviation. Even for a specific case the static calculations described in this paper cannot furnish a complete answer, because from a static point of view a surface with as large an area as possible on a boom as long and flexible as possible without incurring local divergence

would be desirable, whereas from a dynamic point of view these very parameters are those that may have to be avoided. A small area ratio is likely to result in a relatively ineffective lifting surface, whereas a greater ratio is likely to be inefficient, in that the relatively small additional alleviation of static aeroelastic effects which it can produce is likely to be overshadowed by the severity of the dynamic phenomena for which it may be responsible as a result of its greater mass and area. Before an optimum or compromise configuration can be decided upon, several configurations with booms of varying lengths and stiffnesses will therefore have to be analyzed for their static and dynamic aeroelastic characteristics.

CONCLUDING REMARKS

A matrix-integration method has been presented for calculating the static aeroelastic characteristics of a wing with concentrated aerodynamic forces at its tip due to tanks or boom-mounted lifting-surfaces. A simplified method of calculation applicable to certain cases has also been presented, which is based on the concept of the semirigid wing and utilizes the characteristics of the wing alone.

Some static aeroelastic characteristics have been calculated for an unswept wing with a tip tank and for a sweptback wing with several configurations of boom-mounted lifting surfaces. The results of these calculations indicate that a tip tank is likely to affect the static aeroelastic characteristics of an unswept wing adversely and that a boom-mounted lifting surface geared to the aileron tends to relieve the adverse static aeroelastic characteristics of a sweptback wing; the shift of the aerodynamic center and particularly the loss of rolling speed can be reduced in this manner. In the improvement of these characteristics the length and flexibility of the boom are found to be somewhat more effective than the area of the lifting surface. The amount of relief of adverse static aeroelastic phenomena is likely to be limited by dynamic effects introduced by the use of these lifting surfaces, but no such effects have been taken into account.

Langley Aeronautical Laboratory
    National Advisory Committee for Aeronautics
   Langley Field, Va.

REFERENCES

1. Diederich, Franklin W.: Calculation of the Aerodynamic Loading of Swept and Unswept Flexible Wings of Arbitrary Stiffness. NACA Rep. 1000, 1950.

2. Diederich, Franklin W.: Calculation of the Lateral Control of Swept and Unswept Flexible Wings of Arbitrary Stiffness. NACA Rep. 1024, 1951.

3. Diederich, Franklin W.: A Simple Approximate Method for Calculating Spanwise Lift Distributions and Aerodynamic Influence Coefficients at Subsonic Speeds. NACA TN 2751, 1952.

4. Crout, Prescott D.: A Short Method for Evaluating Determinants and Solving Systems of Linear Equations With Real or Complex Coefficients. Trans. A.I.E.E., vol. 60, 1941, pp. 1235-1240.

5. Diederich, Franklin W., and Foss, Kenneth A.: Charts and Approximate Formulas for the Estimation of Aeroelastic Effects on the Loading of Swept and Unswept Wings. NACA TN 2608, 1952.

6. Silvers, H. Norman, and Spreemann, Kenneth P.: Effect of Airfoil Section and Tip Tanks on the Aerodynamic Characteristics at High Subsonic Speeds of an Unswept Wing of Aspect Ratio 5.16 and Taper Ratio 0.61. NACA RM L9J04, 1949.

7. Weissinger, J.: The Lift Distribution of Swept-Back Wings. NACA TM 1120, 1947.

8. Diederich, Franklin W.: Charts and Tables for Use in Calculations of Downwash of Wings of Arbitrary Plan Form. NACA TN 2353, 1951.

TABLE I.- WING PARAMETERS

(a) Unswept Wing

Geometric and structural parameters	Values of parameter with or without tip tank
A	5.16
λ	0.606
Λ	$-1.6°$
c_a/c	0.2
b_a/b	0.5
e	0.40
e_{l_r}	0.255
$(GJ)_r/(EI)_r$	0.8

Aerodynamic parameters	Values of parameter without tip tank	Values of parameter with tip tank
M_0	0.8	0.8
C_{L_α}	4.53	4.97
C_{m_α}	1.16	1.28
κ	0.0963	0.1136
α_δ	0.5	0.5
$C_{L_{\alpha_t}}/C_{L_\alpha}$	------	0.0483
$C_{m_{\alpha_t}}/C_{m_\alpha}$	------	0.0805

(b) Sweptback Wing

Geometric and structural parameters	Values of parameter for subsonic and supersonic flow
A	6
λ	0.5
Λ	$45°$
c_a/c	0.2
b_a/b	0.5
e	0.45
$(GJ)_r/(EI)_r$	0.8

Aerodynamic parameters	Values of parameter for subsonic flow	Values of parameter for supersonic flow
M_0	<0.8	>1.5
κ	0.1030	0.1389
α_δ	0.5	0.2
e_{l_r}	0.20	0

TABLE 2.- DYNAMIC-PRESSURE PARAMETERS AT DIVERGENCE

AND AT AILERON REVERSAL FOR SWEPTBACK WING WITH

BOOM-MOUNTED LIFTING SURFACES

Case	K_v	d/c_t	K	$q*_{BD}$	Subsonic, $q*$		Supersonic, $\bar{q}$	
					Divergence	Reversal	Divergence	Reversal
1	0	----	-	---	-----	0.363	----	5.92
2	.02	0	1	∞	-----	.332	----	5.21
3	.02	1.5	0	∞	0.626	.239	21.7	4.01
4	.02	1.5	1	∞	.626	1.37	21.7	9.22
5	.02	1.5	1	1	.384	1.35	----	----
6	.02	1.5	1	1/2	.277	1.35	----	----
7	.02	1.5	1	1/3	.217	1.34	----	----
8	.02	2.0	1	∞	.409	1.38	14.6	9.76
9	.04	0	1	∞	-----	.312	----	----
10	.04	1.5	1	∞	.312	1.36	----	----
11	.04	2.0	1	∞	.198	3.37	----	----
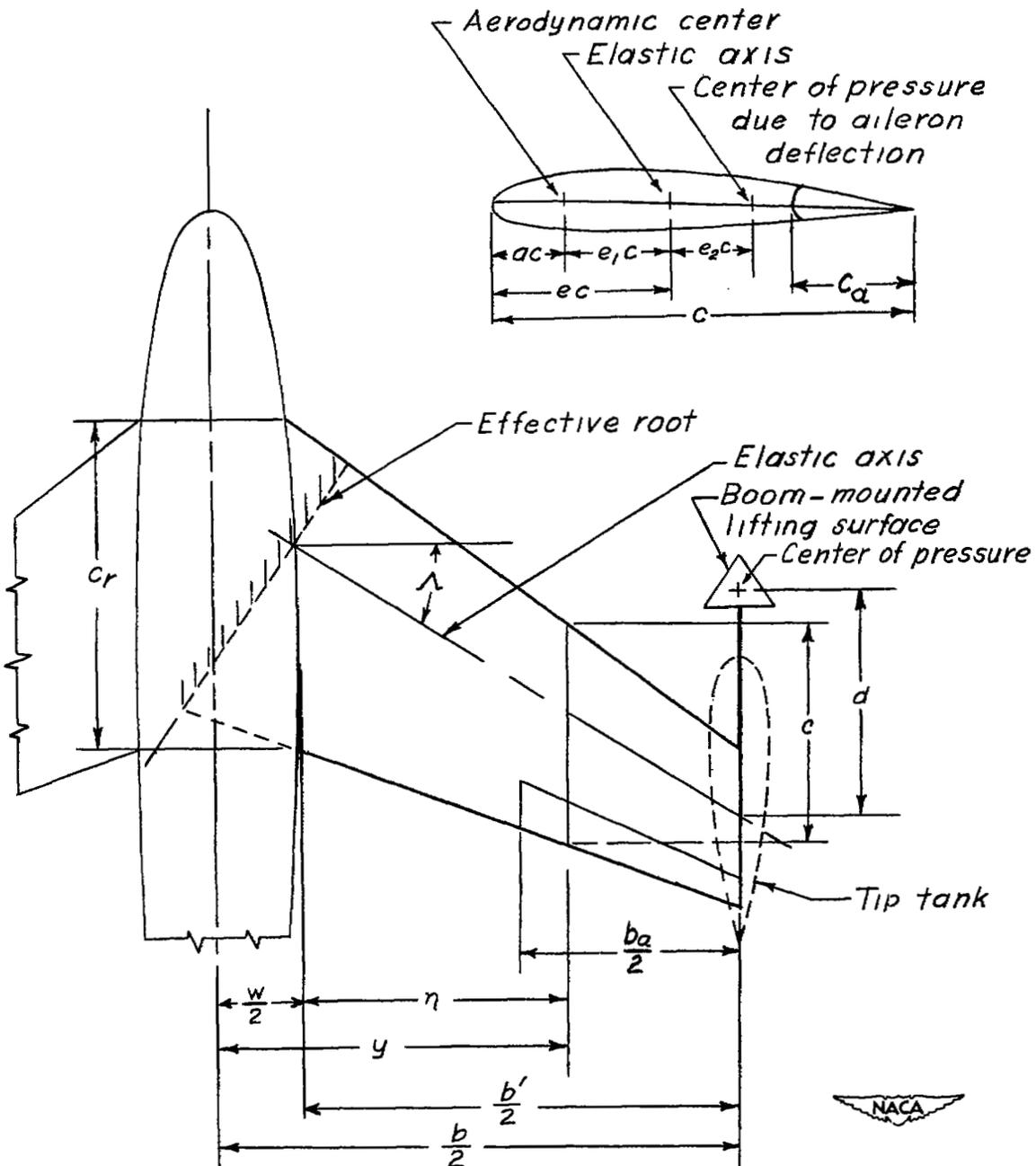
Figure 1.- Definitions of geometric parameters.
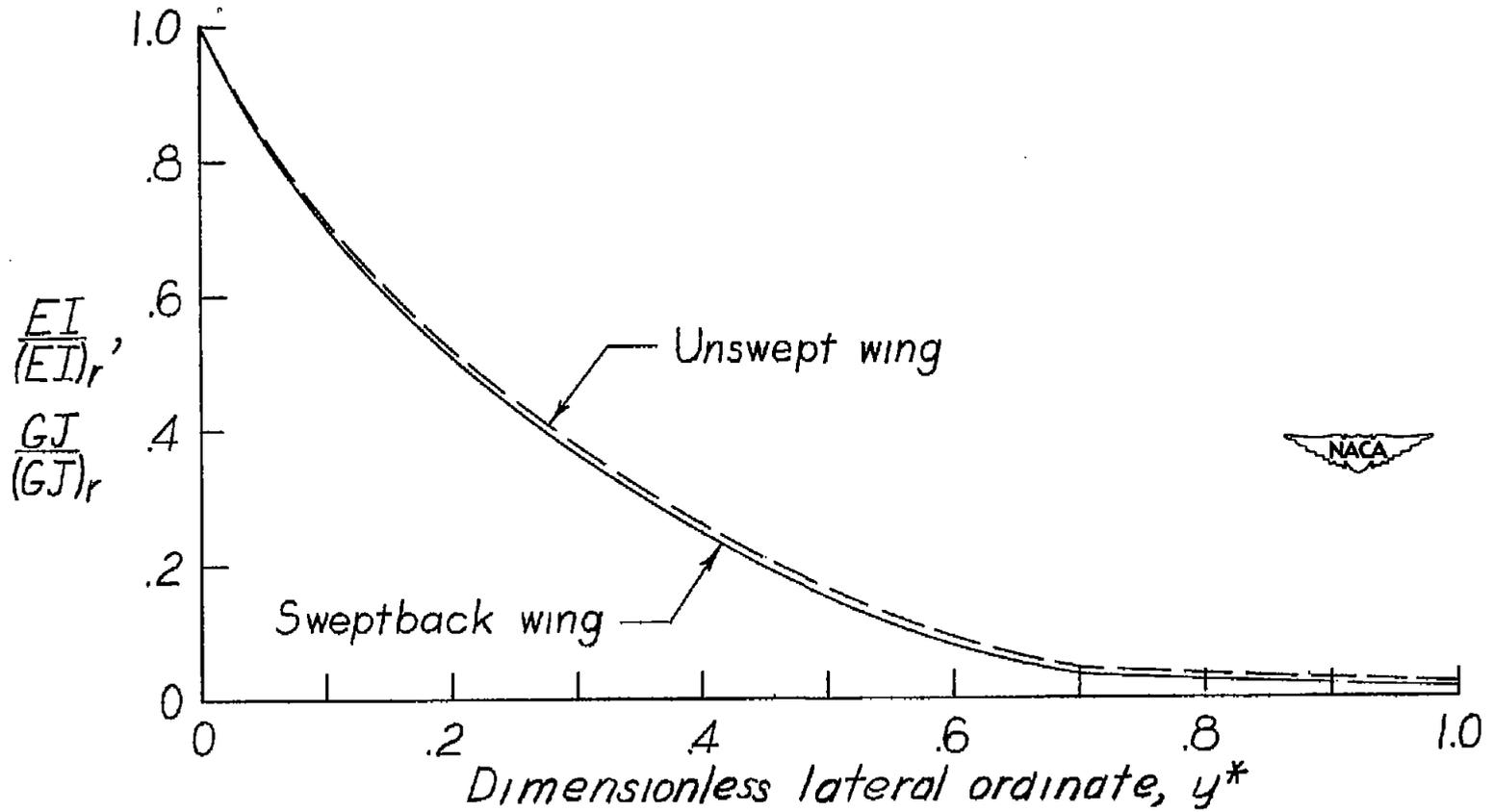
Figure 2.- Stiffness distributions of swept and unswept wings.
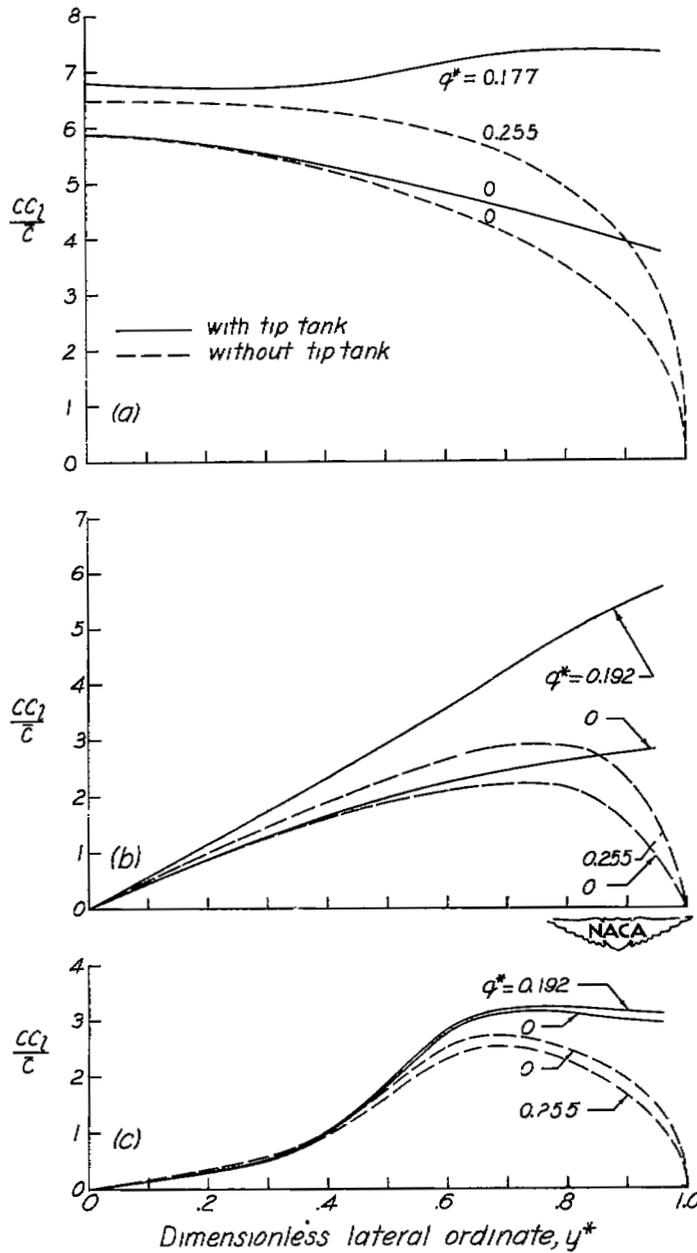
(a) Uniform angle of attack.

(b) Linear antisymmetrical twist (damping-in-roll case).

(c) Aileron deflection ($\alpha_\delta\delta=1$).

Figure 3.- Lift distributions due to uniform angle of attack, linear antisymmetric angle of attack, and aileron deflection for unswept wing. (M = 0.8.)

(a) Unswept wing.
(b) Sweptback wing.
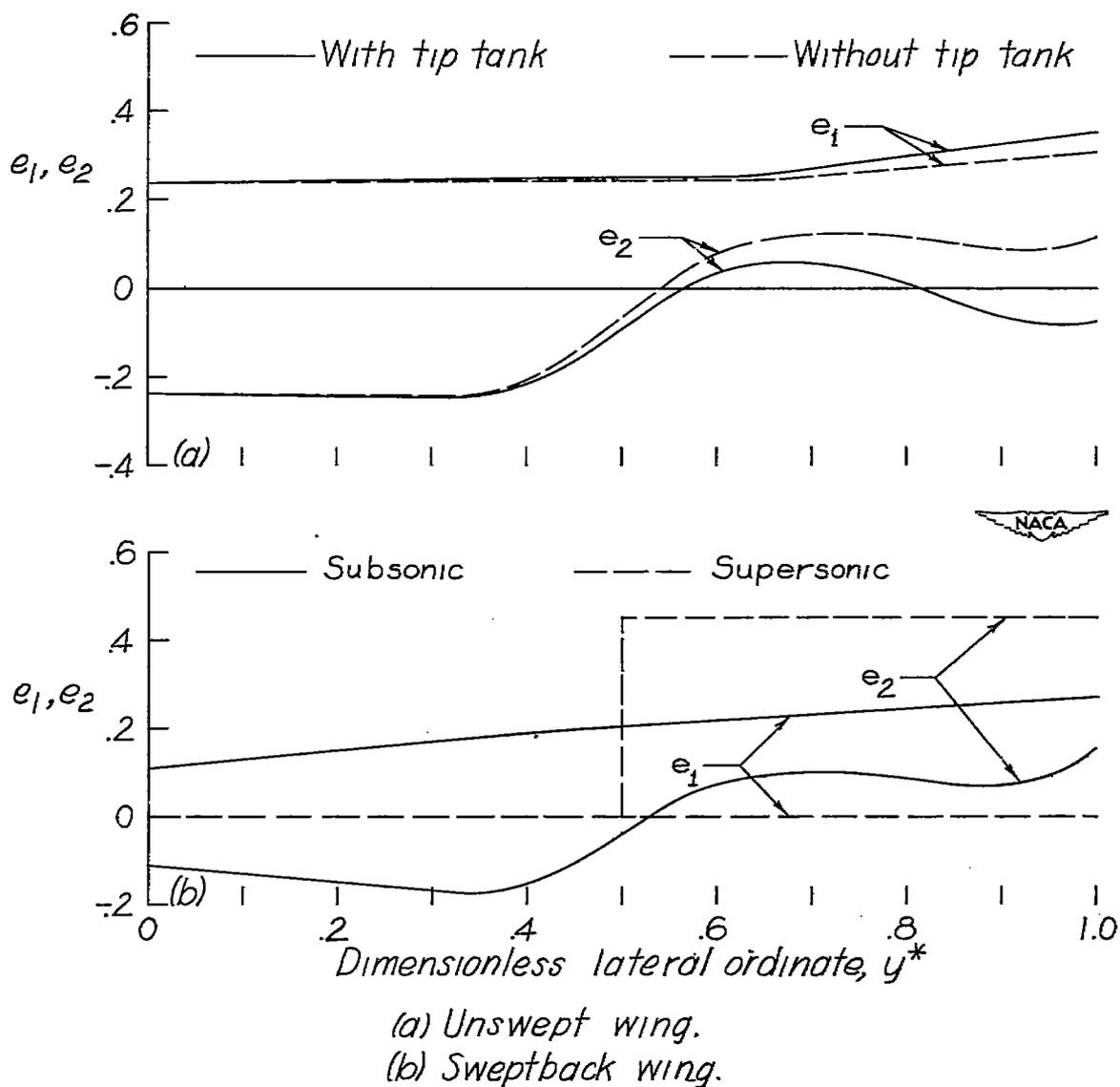
Figure 4.- Spanwise variation of dimensionless moment arms of lifts due to angle of attack and due to aileron deflection for swept and unswept wings.
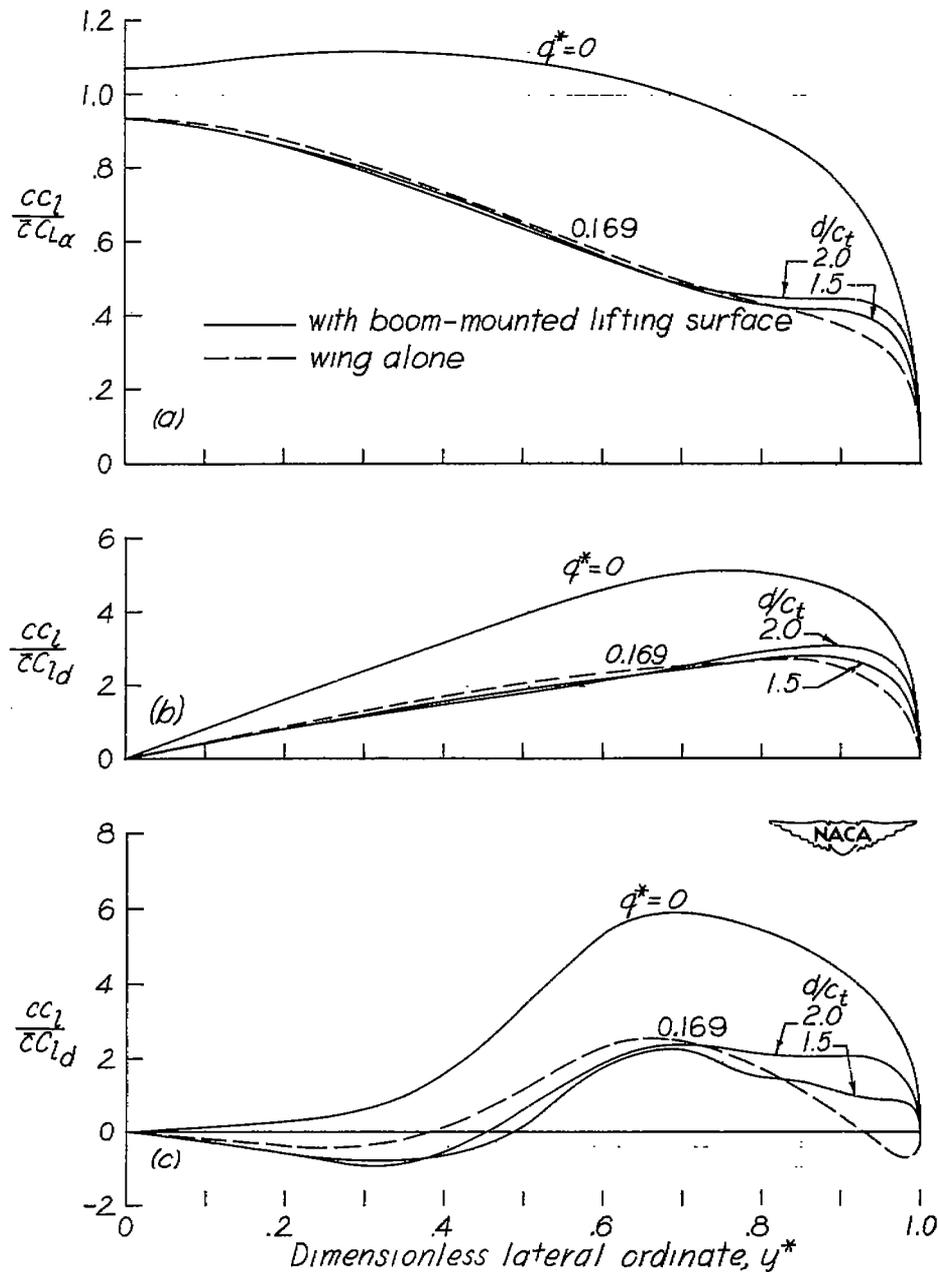
(a) Uniform angle of attack.
(b) Linear antisymmetrical twist (damping-in-roll case).
(c) Aileron deflection ($\alpha_\delta \delta = 1$).

Figure 5.- Lift distributions due to uniform angle of attack, linear antisymmetric angle of attack, and aileron deflection for sweptback wing (subsonic speeds, $K_V = 0.02$).
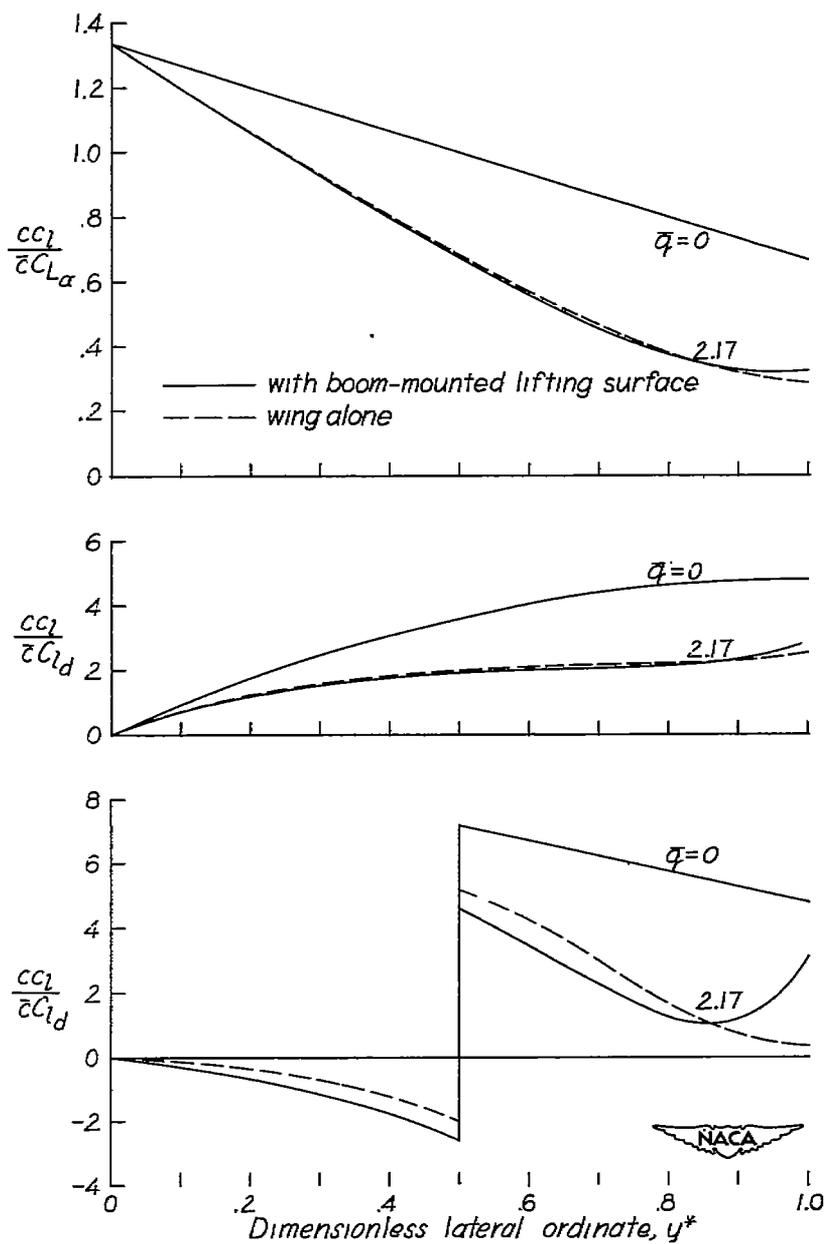
(a) Uniform angle of attack.
(b) Linear antisymmetrical twist (damping-in-roll case).
(c) Aileron deflection ($\alpha_\delta \delta = 1$).

Figure 6.- Lift distributions due to uniform angle of attack, linear antisymmetric angle of attack, and aileron deflection for sweptback wing $\left(\text{supersonic speeds, } K_V = 0.02, \frac{d}{c_t} = 1.5\right)$.
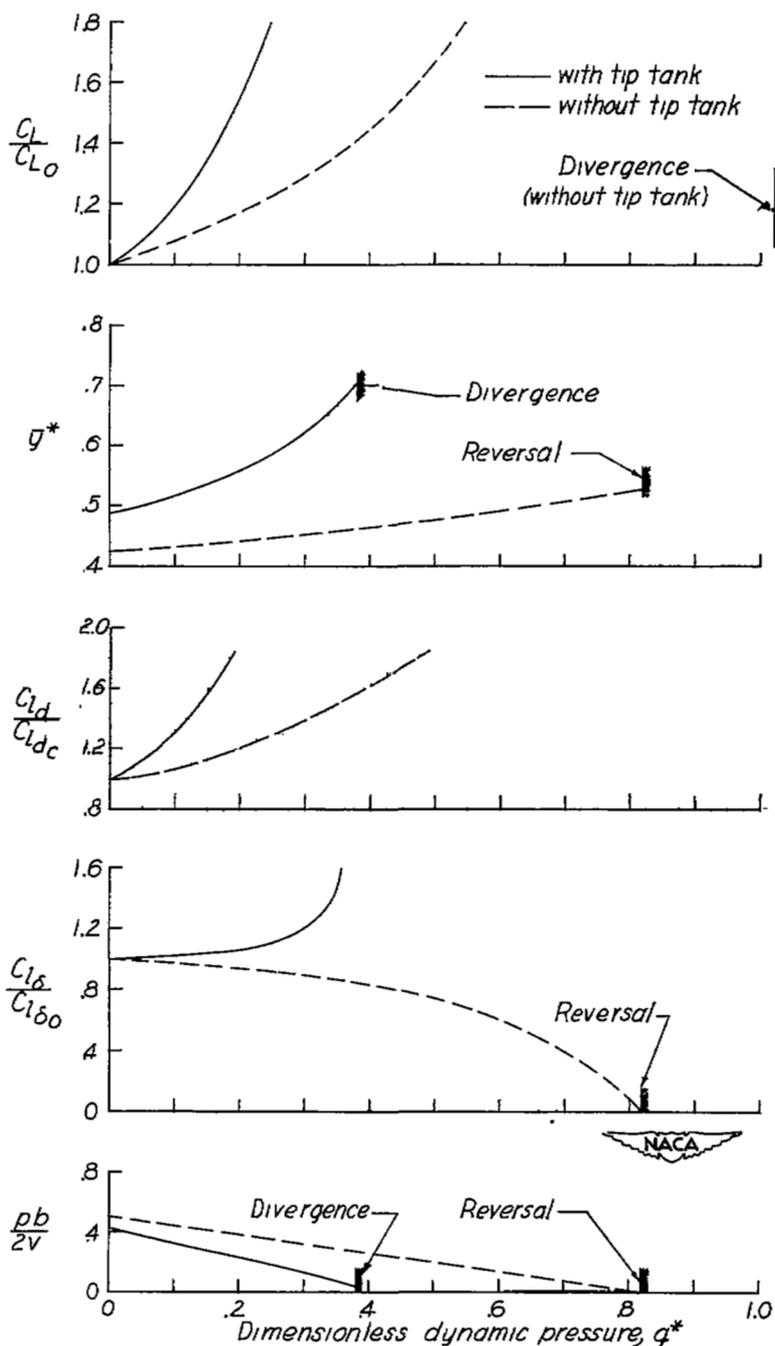
Figure 7.-. Lift-coefficient ratio, lateral center of pressure, damping-in-roll-coefficient ratio, rolling-moment-coefficient ratio, and wing-tip helix angle per unit aileron deflection for unswept wing with and without tip tank (M = 0.8). (Note: q^* is based on C_{L_α} of wing without tank.)
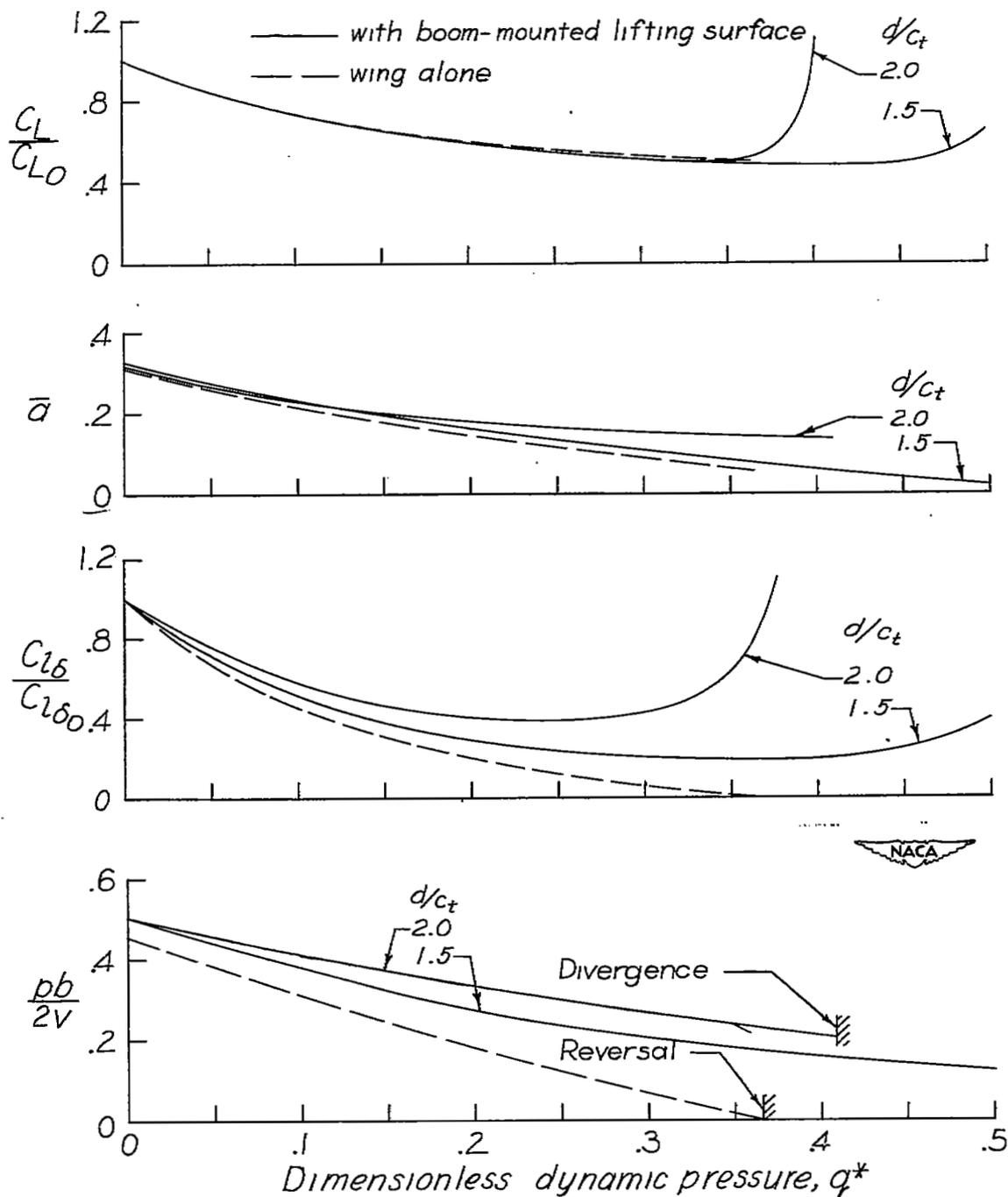
Figure 8.- Lift-coefficient ratio, shift in aerodynamic center, rolling-moment-coefficient ratio, and wing-tip helix angle for swept wing with and without geared boom-mounted lifting surfaces. (Subsonic speeds, $K_v = 0.02$.)
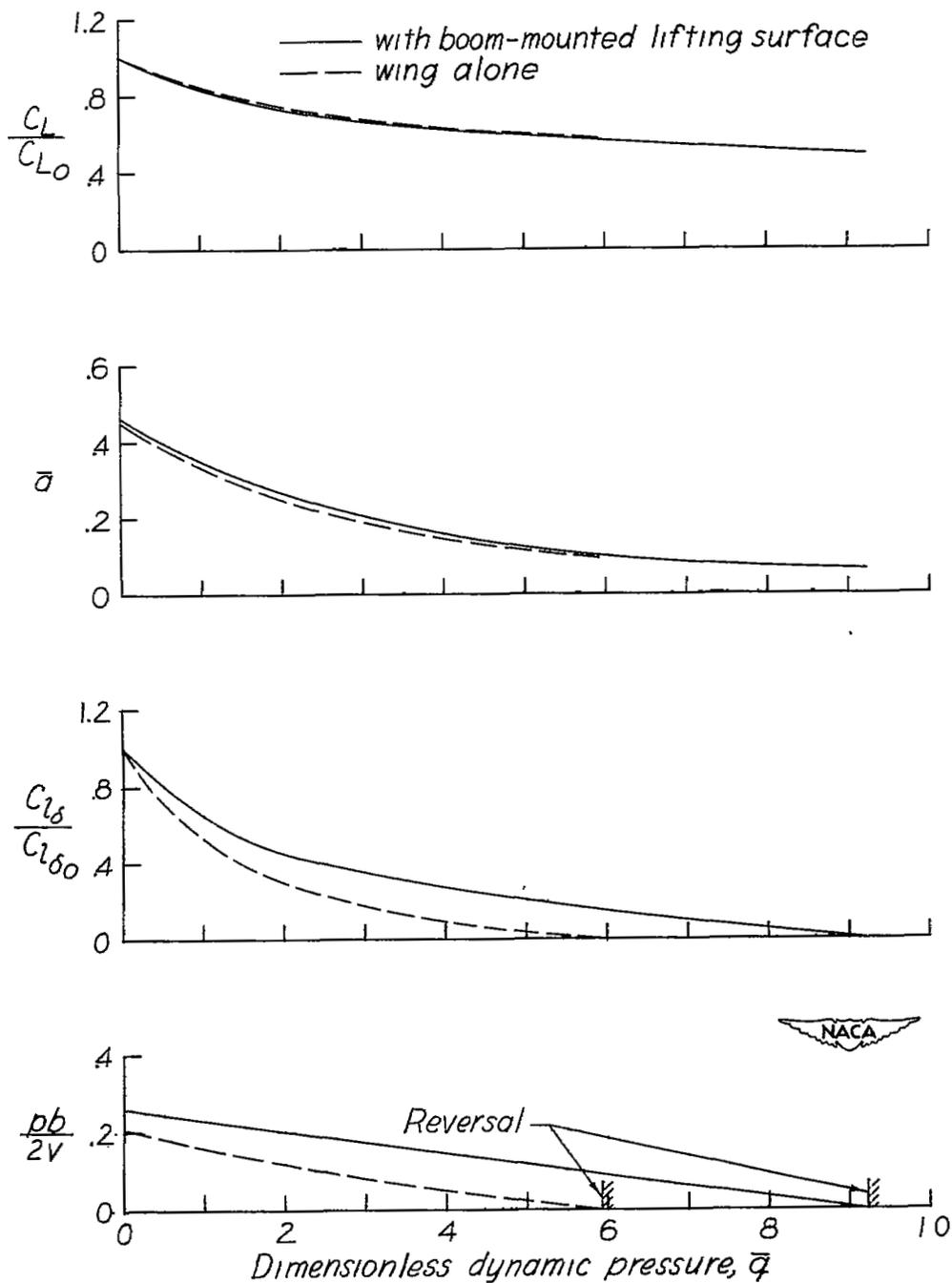
Figure 9.- Lift-coefficient ratio, shift in aerodynamic center, rolling-moment-coefficient ratio, and wing-tip helix angle for swept wing with and without geared boom-mounted lifting surfaces. (Supersonic speeds, $K_v = 0.02$, $\dfrac{d}{c_t} = 1.5$.)
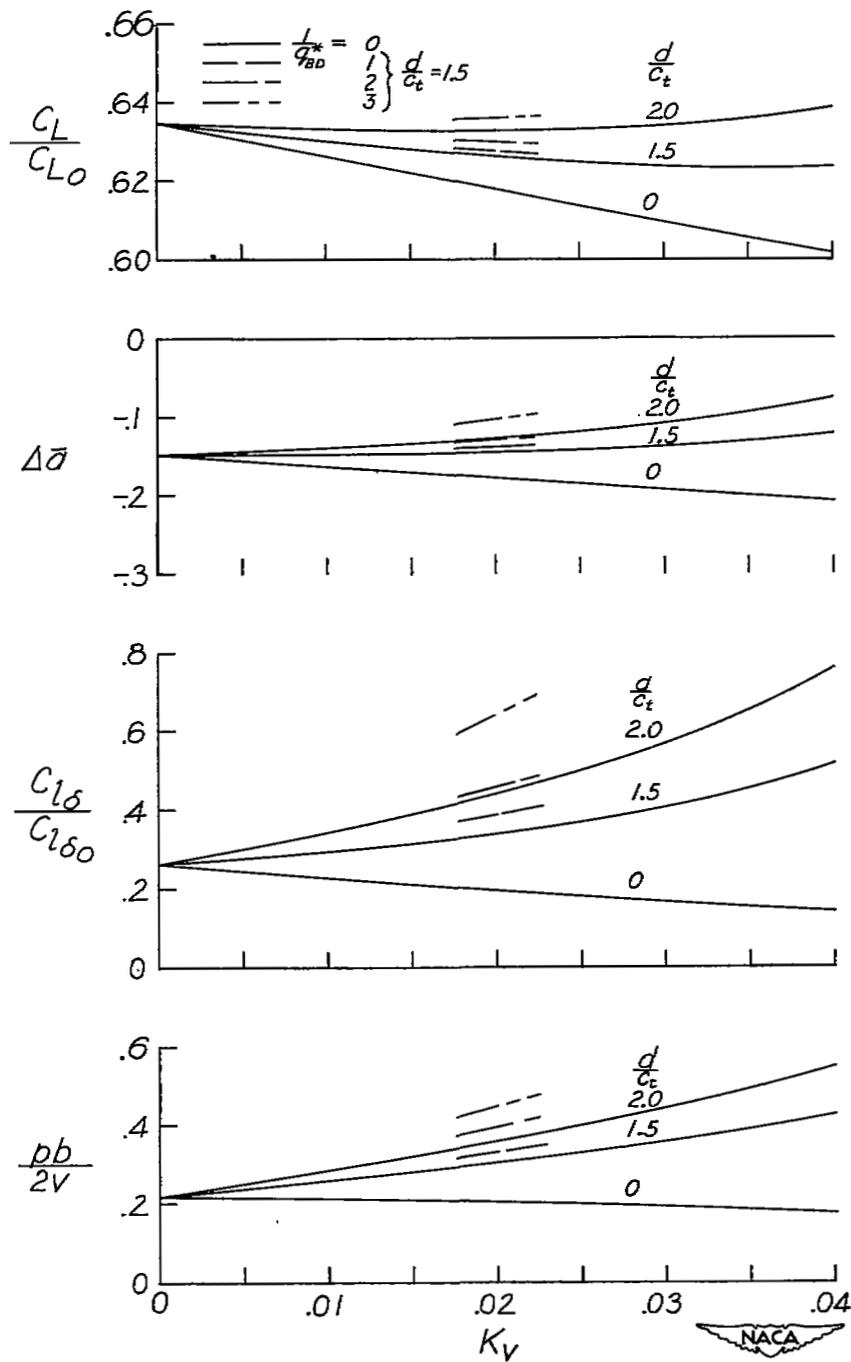
Figure 10.- The effect of lifting-surface size and longitudinal location on the lift-coefficient ratio, aerodynamic-center shift, rolling-moment-coefficient ratio, and wing-tip helix angle for a given dynamic pressure. (q^* = 0.1687, subsonic speeds.)